ELSEVIER

Catalysis Today 58 (2000) 199–230

CATALYSIS TODAY

www.elsevier.com/locate/cattod

Photocatalysis in water environments using artificial and solar light

O.M. Alfano [a], D. Bahnemann [b,*], A.E. Cassano [a,b], R. Dillert [c], R. Goslich [b]

[a] *INTEC, Güemes 3450, 3000 Santa Fe, Argentina*
[b] *Institut fuer Solarenergie-forshung Hameln/Emmerthal (ISFH), Außenstelle Hannover, Sokelantstraße 5, D-30165 Hannover, Germany*
[c] *Ecotransfair, Rebenring 33, D-38106 Braunschweig, Germany*

Abstract

This paper presents a review of part of the work done on photocatalytic reactors. Being aware of the comprehensive reports already existing on the chemistry of these reactions [A.M. Braun, L. Jakob, E. Oliveros, C.A. Oller do Nascimento, Adv. Photochem. 18 (1993) 235; O. Legrini, E. Oliveros, A.M. Braun, Chem. Rev. 93 (1993) 671; D. Bahnemann, J. Cunningham, M.A. Fox, E. Pelizzetti, P. Pichat, N. Serpone, in: G.R. Helz, R.G. Zepp, D.G. Crosby (Eds.), Aquatic and Surface Photochemistry, Lewis Publishers, Boca Raton, FL, 1994, p. 261; M.R. Hoffmann, S.T. Martin, W. Choi, D.W. Bahnemann, Chem. Rev. 95 (1995) 69; D. Bahnemann, in: P. Boule (Ed.), The Handbook of Environmental Chemistry, Part I, Vol. 2, Environmental Photochemistry, Springer, Berlin, 1999, p. 285] we have focused our work on two main themes: (i) light absorption evaluation when artificial light is used and (ii) description of reactor configurations and applications when solar radiation is employed. A classification is proposed for both topics and typical examples have been chosen to illustrate the specified concepts.

Keywords: Photocatalytic reactor; Artificial light; Solar light; Reactor modelling; Reactor engineering; Photocatalysis

---

1. Introduction

Almost 20 years ago photocatalytic reactions irrupted into the scientific literature when they were proposed as a suitable way to promote the separation of molecular hydrogen and molecular oxygen from water using solar illumination [6–8]. In the mid-1980s the economic feasibility of this process was questioned and, unfortunately, no significant progress has been made ever since. Almost at the same time, a second attractive application was proposed; several papers published by Ollis' group [9–12] among others indicated that a similar approach could be used for degrading organic compounds present in water or air streams.

Photocatalysis by semiconductors is the result of the interaction of electrons and holes generated in an activated solid with the surrounding medium. Activation is the consequence of light absorption; thus, electron–hole pairs are formed in the solid particle that can recombine or participate in reductive and oxidative reactions that lead to the decomposition of contaminants. One of the concepts that has received an increasing degree of attention has been the use of titanium dioxide as a catalyst for the light induced degradation of pollutants [13–18].

The degradation of many different model compounds has been studied and it has been clearly shown that most of the organic pollutants present in water can be fully decomposed [19–22]. Halogenated hydro-

---

[*] Corresponding author. Tel.: +49-511-3585-0137; fax: +49-511-3585-0110.
E-mail address: isfh.bahnemann@oln.comlink.apc.org (D. Bahnemann)

0920-5861/00/$ – see front matter
PII: S0920-5861(00)00252-2

carbons, aromatic hydrocarbons, nitrogen-containing heterocycle compounds, hydrogen sulfide, surfactants, herbicides, metal complexes and many other compounds have been examined, particularly in water solution [23].

Photocatalytic reactors differ from the more conventional ones (of thermal or thermal-catalytic nature) by the presence of a radiation field that produces the activation of the catalyst. The catalyst most widely employed, titanium dioxide, absorbs radiation below the visible range of the light spectrum; hence at least near UV light is needed. The light that gives rise to the required radiation field can be produced by artificial lamps or by solar irradiation. In both cases, the optimization of this light activated step is, together with the catalyst selection, very likely to be the key point for the design of these reactors.

Though its fully destructive characteristics make this process a very attractive oxidation technology, several questions remain to be answered regarding the economical competitiveness of large-scale applications. At the same time, research has yet to succeed in developing a comprehensive and sound understanding and description of all the involved phenomena, with the challenge reaching its maximum manifestation when real wastewater and varying solar illumination become the implicated issues.

Photocatalytic reactions and its applications have been recently reviewed in several comprehensive papers [1–5]. In order to keep the length of this work within reasonable bounds we have concentrated this review in two main matters: (i) when artificial light is used, an analysis of the different proposed methods to evaluate light absorption, as part of the attempt to produce suitable quantitative results for reactor design and (ii) when solar illumination is employed, a description of the most significant reactor configurations, considering that from the economical viewpoint, this may be the most attractive application.

2. Photocatalytic reactors using artificial light

There are three central problems in designing a photocatalytic reactor: (1) the analysis of the reaction (paths, mechanisms, products, efficiencies, etc.) together with the choice of the most efficient catalyst; (2) the analysis of the reaction kinetics and of the methods for reactor design for different reactor geometries and (3) the provision of adequate irradiation for the whole reactor volume. The first problem, as indicated above, has been exhaustively addressed in previous reviews [1–5]. An examination of the most important aspect related to the second one is dealt with in a paper published in this issue [24]. For the third, evaluation of light absorption and development of reaction kinetic expressions (that explicitly include true radiation absorption effects) are needed. This part of the paper will mainly concentrate on this very distinctive aspect of photocatalytic reactors and with this objective a short description of some representative work extracted from the international literature will be presented. Purposely, we have not included a long list of references with all the published work, but only typical examples of the different approaches that have been used in the past, so as to be able to focus on the discussion of the different proposals and the underlying concepts.

A previous review on radiation models for heterogeneous photochemical reactors was written by two of the authors back in 1986 [25] and this information will not be repeated here. The work reviewed here has been summarized in Tables 1 and 2.

Hereafter, the different methods that have been used to analyze the results of photocatalytic reactors activated by artificial UV radiation (UV lamps) are briefly described. We will consider two main approaches: (i) those based on different types of theoretical analyses using the radiative transfer equation (RTE) that led to simplified or rigorous mathematical models and (ii) those based on experimental design.

2.1. Using the radiative transfer equation

Since radiation absorption is the single, most distinct characteristic of photocatalytic reactors it is possible to classify the most significant contributions to that form of quantitative work that can be useful for reactor design, according to the way in which this process is considered. With this purpose, let us look at the radiative transfer equation (RTE) in its most general formulation. Four processes may be present: emission, absorption, out-scattering and in-scattering (resulting from multiple scattering) [26]:

Table 1
Analysis of photocatalytic reactors using the RTE

Main characteristics	Applications	References
Scattering phenomena not modeled		
Radiation flux measurements at the reactor wall of radiation entrance using detectors or actinometers	Water photolysis in aqueous suspension of TiO_2 particles, annular photoreactor	Esplugas et al. [28]
	Evaluation of radiant energy absorption in aqueous TiO_2 dispersion	Schiavello et al. [29], Augugliaro et al. [30]
	Photocatalytic degradation of phenol in aqueous suspension of TiO_2 particles	Yue [31]
	Quantum and chemical yields of photocatalytic reactions	Pichat [36]
Homogeneous chemical actinometry	Degradation of benzene and perchloroethylene by photoassisted heterogeneous catalysis over TiO_2	Turchi and Ollis [38]
	Quantum yield of the photocatalytic chloroform degradation. Influence of radiation, temperature and pH	Bahnemann et al. [40]
Photocatalytic reactors having mass transfer limitations	Phenol degradation over TiO_2 catalyst in a continuous annular photoreactor	Sclafani et al. [41]
Modeling scattering phenomena		
Zero reflectance and Two-flux models	Radiative flux measurements of aqueous suspension of TiO_2 particles	Brucato and Rizzuti [42,43]
Random-walk model	Chemical actinometry with plastic beads, porcelain particles and Toyura sands photocatalytic reduction of Cr(VI) with suspended TiO_2 particles	Yokota et al. [44–46], Cervera et al. [47]
Radiant field simulations with Monte-Carlo technique	Radiative flux measurements at the outer wall of an annular reactor. Aqueous suspension of TiO_2 particles	Pasquali et al. [48]
Solution of the RTE neglecting scattering-in	Photocatalytic decomposition of chloroform in aqueous suspension of TiO_2 kinetics and quantum efficiencies	Martin et al. [50–52]
Solution of the complete RTE using the discrete ordinate method	Chemical actinometry with spherical particles of pure silica decomposition of trichloroethylene in water solution	Alfano et al. [53,55], Cabrera et al. [54,56],
	radiation field inside a flat-plate photocatalytic reactor	Brandi et al. [59,60],
	radiation field inside an annular photocatalytic reactor	Romero et al. [61]

$$\frac{\mathrm{d}I_\lambda(s,\underline{\Omega},t)}{\mathrm{d}s} + \underbrace{\kappa_\lambda(s,t)I_\lambda(s,\underline{\Omega},t)}_{\text{Absorption}} + \underbrace{\sigma_\lambda(s,t)I_\lambda(s,\underline{\Omega},t)}_{\text{Out-scattering}} = \underbrace{\dot{j}_\lambda^{\,\mathrm{e}}(s,t)}_{\text{Emission}} + \underbrace{\frac{1}{4\pi}\int_{\Omega'=4\pi}\int_{\lambda'=\lambda_1}^{\lambda'=\lambda_2}\sigma_{\lambda'}(s,t)\, p(\underline{\Omega}'\to\underline{\Omega},\lambda'\to\lambda)\, I_{\lambda'}(s,\underline{\Omega}',t)\,\mathrm{d}\lambda'\,\mathrm{d}\underline{\Omega}'}_{\text{In-scattering}} \qquad (1)$$

Normally, with the exception of work performed at high temperatures, emission can be safely neglected; hence, it will not be considered for the case of photocatalytic reactions in water systems. The first two terms constitute the well-known Lambert–Beer equation for homogeneous media. When catalytic particles are present, the participating medium is macroscopically heterogeneous and scattering becomes impor-

Table 2
Use of experimental design in photocatalytic reactors

Main characteristics	Applications	References
Optimal experimental design	Pilot level titanium dioxide photocatalyzed oxidative degradation of organic pollutants contained in industrial wastewaters	Jakob et al. [62], Braun et al. [1]
Neural networks	Large-scale actinometry in a continuous elliptical photochemical reactor with a concentric annular reaction chamber, chemical actinometer: photosensitized decomposition of an uranyl oxalate homogeneous solution	Braun et al. [1]
	Photocatalytic degradation of wastewater pollutants in a multi-lamp immersion-type photoreactor; experimental points and neural network simulated curves for different conditions	Jakob et al. [62]
Empirical approximations	Proposal of novel reactor configurations. Evaluation of reactor performances	Mukherjee and Ray [65]

tant. The RTE is still a simple ordinary differential equation if in-scattering is neglected. However, the scattering coefficient $\sigma_\lambda(s,t)$ cannot be easily measured with the same techniques employed in homogeneous spectrophotometry [27] and consequently even out-scattering is difficult to compute. Then, it is of no surprise that much work has been performed without a quantitative consideration of scattering. Even if the scattering coefficient is known, in-scattering turns the RTE into an integro-differential mathematical form that is not amenable to analytical solutions for practical cases and difficult to solve numerically. Hence, only few groups have included the complete RTE in their studies of photocatalytic reactions and reactors.

When Eq. (1) is solved from the values of $I_\lambda(s, \underline{\Omega}, t)$ the local volumetric rate of radiation energy absorption (LVREA, point valued radiation absorption rate per unit reaction volume) can be readily obtained

$$e^{\mathrm{a}}(\underline{x}, t) = \int_\lambda e_\lambda{}^{\mathrm{a}}(\underline{x}, t)\,\mathrm{d}\lambda = \int_\lambda \kappa_\lambda(\underline{x}, t) G_\lambda(\underline{x}, t)\,\mathrm{d}\lambda = \int_\lambda \kappa_\lambda(\underline{x}, t) \int_{4\pi} I_\lambda[s(\underline{x}, \underline{\Omega}), \underline{\Omega} t]\,\mathrm{d}\Omega\,\mathrm{d}\lambda \qquad (2)$$

Looking at Eq. (1) an obvious and direct way of classifying the work that includes some sort of theoretical modeling is to divide these contributions in two groups: (i) studies that do not include the modeling of scattering and (ii) studies that include the representation of scattering. In each of these groups the analyses made by different authors have a wide range of approximations and/or mathematical complexities.

2.1.1. *Scattering phenomena not modeled*

When scattering is not modeled, two main approaches have been used: (1) radiation flux measurements at the reactor wall of radiation entrance and (2) homogeneous actinometry inside the reactor as it is usually done with homogeneous reactions. In the first case, two different experimental techniques have been reported: (1.1) using radiation detectors of different types; (1.2) using homogeneous actinometry. Recognizing that these are not proper measurements of the absorbed radiation by the photocatalyst, it is usually stated that results obtained from these techniques provide only an approximation, which constitutes some sort of an upper limit for computing absorbed radiation. In this group of papers, and for completeness, we have also included some studies on reactors that have not modeled scattering and have been mainly devoted to the analysis of a system with mass transfer limitations (Table 1).

With respect to the group of papers that have employed radiation flux measurements we can mention first one study of Esplugas et al. [28]. They have made an experimental investigation of the water photolysis reaction in a batch annular reactor; the catalyst employed was $RuO_2/Pt/TiO_2$. Two types of actinometric measurements were performed: (i) placing one uranyl oxalate actinometer inside the reactor in order to measure the radiation flux entering the reactor from the top (also the lamp emission per unit lamp-length) combined with (ii) locating another actinometer (potassium ferrioxalate) in different positions around the reactor external wall and at the reactor bottom to evaluate the non-absorbed radiation escaping from all these reactor walls. With this system the radiation absorption rate by the photocatalytic mixture was estimated; they reported an apparent (minimum) overall quantum yield of 0.00165 mol Einstein^{-1} for the production of molecular hydrogen.

Schiavello et al. [29] and Augugliaro et al. [30] also proposed an experimental technique to measure the radiation flux absorbed and reflected-out by an aqueous suspension of different titanium catalysts. A small cylindrical reactor was used; the sides of the walls were covered with aluminum foil (to reflect back into the reactor the out-scattered radiation). Actinometry was used to measure the incoming radiation at the wall of radiation entrance and the outgoing radiation at the opposite face of the reactor. They proposed the following radiation balance for the reactor:

$$q_\mathrm{i} = q_\mathrm{a} + q_\mathrm{r} + q_\mathrm{t} \tag{3}$$

In Eq. (3) q_i is the radiation flux entering the reactor at the top, q_a the absorbed radiation by the solid suspension inside the reactor, q_r the reflected radiation at the reactor top and q_t the transmitted radiation through the reactor bottom. The authors measured q_i and q_t for different operating conditions; from these results they evaluated q_r and q_a. This method was then applied to the analysis of the photocatalytic degradation of phenol in a batch reactor under different experimental conditions and using different types and brands of catalysts.

In 1993, Yue [31] proposed a method to evaluate radiation absorption in a photocatalytic reactor and applied it to an annular reactor (the lamp placed at the reactor's central axis). He used a silicon photodiode connected to a radiometer/photometer. The following measurements were carried out: (i) at the inner wall of the reactor (M_0); (ii) at the outer wall of the reactor having the reaction mixture without the catalyst inside (M_1) and (iii) at the outer wall of the reactor having the complete reacting suspension inside (M_2). The volumetric rate of energy absorption was calculated according to

$$e^\mathrm{a} = \frac{A_\mathrm{in}\phi\alpha M_0}{V} \tag{4}$$

where α is a constant that relates the incident radiation (Einstein m^{-2} s^{-1}) with the radiation flux (W m^{-2}) and ϕ is the fraction of the light absorbed by the catalytic particles; ϕ was calculated according to

$$\phi = \frac{A_\mathrm{ou}(M_1 - M_2)}{A_\mathrm{in}M_0} \tag{5}$$

This method was used to study the photocatalytic decomposition of phenol in water using Degussa P25 titanium dioxide. A batch, annular photoreactor was employed having a tubular, actinic type lamp inside. Lea and Adesina [32] and Dadydov et al. [33] have used similar methods. This approach — or minor modifications of it — has been widely used according to the reports in the literature dealing with photocatalytic reactions; another typical and very recent example is the work of Rideh et al. [34].

Even if not directly related to light evaluation procedures, a good addition to the understanding of the liquid phase operation of these catalytic systems is the proposal of an approximate method for the analysis of photocatalytic reactors that has been presented by Ollis and Turchi [35]. They have not taken into account scattering (they use Lambert–Beer's equation for homogeneous systems instead) and, consequently, this may be an appropriate place to include their contribution. The paper summarizes current rate equations for the photocatalytic destruction of multiple water pollutants as well as simplified convective transport equations that are based on a rather simplified analysis. The authors consider this approach to be appropriate for photocatalytic reactor design. They also describe an approximate method for treating simultaneous heterogeneous (photocatalyzed) and homogeneous (photolytic) reactions. Published in 1990, this is the first paper — that we know of — that has proposed one photocatalytic design method based on the fundamentals of chemical reaction engineering.

A different approach was presented in a review paper by Pichat [36]. This work concerned the photocatalytic oxidation of organic compounds in aqueous and organic liquid phases. Pichat presented an analysis of several aspects of these reactions; among them the measurement of photocatalytic quantum yields defined as the ratio of the number of desired product molecules produced in the reaction and the radiation quanta absorbed by the photocatalyst. According to Pichat, the absorbed radiation can be calculated from

$$n_\mathrm{a} = n_\mathrm{ph}(q_\mathrm{i} - q_\mathrm{t})(1 - R) \tag{6}$$

Here n_ph is the number of photons that could be absorbed by the catalyst (calculated from the catalyst absorbance values, the spectral distribution of the lamp emission power and the spectral transmission of the employed filters), q_i the incident radiation flux (measured with a calibrated photometer), q_t the transmitted radiation flux and R is the catalyst reflectivity. The same author had proposed a similar approach several years before [37].

The second group listed in Table 1 considered that the absorbed radiation is that resulting from a properly performed homogeneous actinometry inside the reactor. A typical representation is the work of Turchi and Ollis [38]. They have used this method to evaluate the absorbed energy in an annular reactor irradiated with seven UV lamps (one at the reactor's central axis and the other six surrounding the external wall). Potassium ferrioxalate was the actinometer. As the authors indicated, this method overestimated the absorbed radiation energy because: (i) it does not account for the loss of photons produced by scattering and (ii) the used actinometer collects all the emitted radiation but the catalyst only absorbs energy below 380–390 nm. This approach was applied to the mineralization of a binary reacting system containing perchloroethylene (PCE) and benzene in water using Degussa P25 titanium dioxide as the photocatalyst. The initial reaction rate data were well represented by a mathematical equation equivalent to Langmuir–Hinshelwood kinetics. Apparently PCE decomposed without significant concentrations of reaction intermediates while the interpretation of the kinetic data from the benzene oxidation demanded the inclusion of a minimum of two reaction intermediates. Important interferences were also observed: relatively high concentrations of benzene produced a retarding effect on the PCE decomposition while the presence of PCE had almost no effect on the benzene oxidation rate. A similar approach had been used in the past by Pruden and Ollis [39] to study the complete mineralization of trichloroethylene in water employing titanium dioxide and a reactor having the same characteristics as the one used by Turchi and Ollis [38]. When used for estimating quantum efficiencies, results obtained with this method have usually been named: "apparent" values.

The same method was also used by Bahnemann et al. [40] when they studied the photocatalytic decomposition of chloroform in aqueous solution with Degussa P25 being the photocatalyst. They employed a different actinometer: Aberchrome 540 in order to evaluate radiation absorption in the range 310–370 nm exclusively. These measurements were used to investigate the effect of radiation intensity (actually the incident radiation) on the reaction rate. Within the explored range of experimental variables and at pH=7.2 a square root dependence of the reaction rate on the incident radiation was observed. The effect of incident radiation, pH and temperature were also studied; these findings were reported in terms of the overall quantum yield for the chloroform degradation. Under low irradiating conditions (absorbed radiation $<10^{-6}$ Einstein L^{-1} s^{-1}) the overall yield increased with increasing pH. On the other hand, for rather high values of the absorbed radiation ($>6\times10^{-5}$ Einstein L^{-1} s^{-1}) the overall yield was low and almost insensitive to changes in pH. For rather high values of radiation absorption a negative temperature coefficient was observed, i.e., the reaction rate decreased with increasing temperature.

The third group classified in Table 1 corresponds to the case of photocatalytic reactors that undoubtedly worked under mass transport limitations. A typical example is represented by a contribution of Sclafani et al. [41]. They studied the oxidation of phenol and employed TiO_2 in a fixed bed, continuous, annular photoreactor irradiated by a high-pressure mercury UV lamp. The employed catalyst consisted of large particles (average diameter=0.12 cm) of the anatase variety of titanium dioxide. Experiments were made for different phenol concentrations and several flow rates. The reaction rate was found to be strongly dependent on the feed flow rate, i.e., reactant diffusion played an important role in the process kinetics; then, the authors concluded that under all their experimental conditions the reaction was controlled by mass transport. The interpretation of the results was made with a simple model that accounts for phenol and oxygen mass transport from the liquid to the solid. For low phenol concentrations the mass transfer limitation corresponded mainly to phenol slow diffusion. On the other hand, for high phenol concentrations the mass transport limitation was clearly due to a lack of the required amount of molecular oxygen at the reaction site.

2.1.2. *Modeling the scattering phenomena*

In this case we can distinguish four groups of contributions: (i) simplified models; (ii) a random-walk model; (iii) radiation field simulation with Monte-Carlo techniques and (iv) solution of the RTE using the discrete ordinate method (DOM).

Two simplified models were presented in a two-part paper by Brucato and Rizzuti [42,43]: the first is a zero-reflectance model and the second a two-flux model. Both models are representative of two limiting conditions for the photon-particle interaction. The authors have considered that when a photon impinges on the surface of a catalytic particle one can have: (i) total absorption (zero-reflectance model) and (ii) reflection in a purely back scattering direction (two-flux model). It should be noted that notwithstanding that the zero-reflectance approach does not model scattering it has been included in this group because it may give an approximate representation for the case of negligible scattering. Both models lead to very simple formulations that are amenable of analytical solutions. These models, even if obtained with rather unrealistic assumptions, provide simple results for first order estimates in photocatalytic reactor design. The first model overestimates the photon absorption rate (all the impinging energy is absorbed) and the second underestimates the photon absorption rate because it computes reflection (a sort of macroscopic scattering) with its maximum influence. Since each of the models represents almost opposite situations, it is stated by the authors that the real performance of a heterogeneous system may lie somewhere between both predictions.

Yokota et al. [44] proposed a random-walk model for describing scattering in a liquid–solid system. Results were obtained with Monte-Carlo simulation to evaluate the radiant energy distribution inside the reactor. The model incorporated two adjustable parameters that represented anisotropic scattering and absorption by the solid particles. This proposal was based on the following assumptions: (i) the reaction space is divided into many small cubes of equal volume; each cube contains only one particle and consequently the probability of the photon–particle interaction is uniform; (ii) one photon can travel exclusively along the six directions corresponding to a three-dimensional Cartesian coordinate system and (iii) anisotropic scattering is accounted for by assigning to one direction a given probability of traveling and a different — but equal — probability to all the other five remaining directions. The model was applied to a cubic reactor; radiation entered through one face; using a potassium ferrioxalate actinometer solution the scattered radiation through the opposite and lateral faces was measured. Different scattering centers were used: spherical transparent plastic beads, white opaque porcelain particles and brownish translucent sands. This work was published simultaneously with a direct application to a photo-oxygenation reaction [45]. The random-walk model was applied to evaluate the influence of the photon absorption rate on the oxidation of 2,3-dimethyl-2-butene using dye-supported solid particles as photosensitizers. Afterwards, Yokota et al. [46] proposed mathematical correlations to relate the two adjustable parameters to the optical properties of the liquid and the solid particles. Finally, Cervera et al. [47] used the random-walk model to estimate the radiation absorption rate when they studied the photocatalytic reduction of Cr(VI) employing an aqueous suspension of Degussa P25 titanium dioxide. This work was carried out in the laboratory (with a Xe lamp) and in pilot plant size with solar radiation (“Plataforma Solar de Almería”, Spain).

In 1996 Pasquali et al. [48] published a rigorous work that deals with the simulation of the radiation field inside a photocatalytic reactor. This research followed a previously published theoretical paper from the same group [49] that constitutes the first attempt to apply fundamental radiation transport theory to heterogeneous photochemical systems. Pasquali et al. evaluated the radiation field in a cylindrical, two-dimensional, participative and reacting medium, where absorption and scattering coexist. An annular, continuous photocatalytic reactor, having a tubular UV lamp at its central axis was studied (Fig. 1). The lamp was modeled as a linear source with diffuse emission. Scattering at the particles was considered specular or diffuse, giving rise to the application of two different phase functions: (i) the isotropic specular distribution and (ii) the diffuse distribution (anisotropic with preferential scattering to the back). To avoid the complete solution of the RTE (Eq. (1)) in curvilinear coordinates, the authors used direct simulation with the method of Monte-Carlo. The objective was to calculate the LVREA at every point inside the reaction space. Essentially, this method consists in following a statistically significant number of photon beams from their emission point (the lamp) until they are either absorbed by the solid or escape from the

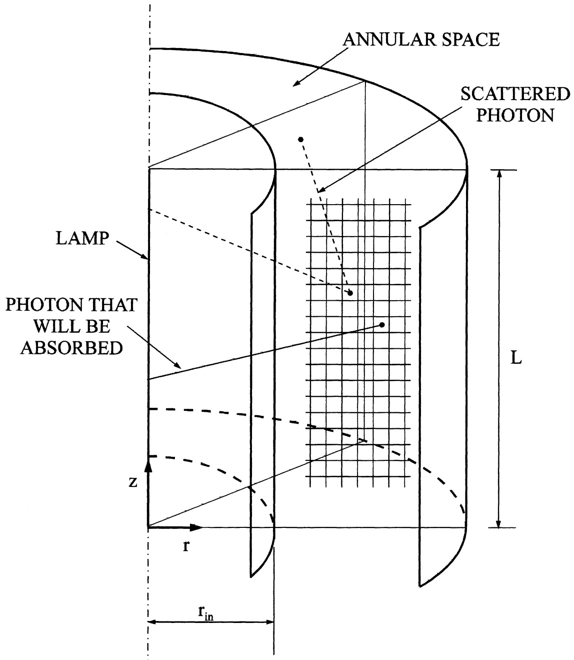

Fig. 1. Schematic representation of Monte-Carlo method of calculation for the modeling of an annular photocatalytic reactor. (adapted from Spadoni et al. [49]).

reactor boundaries due to successive scattering by the particles. Pasquali et al. [48] found that the value of the optical thickness of the system ($(\sigma+\kappa)\Delta s$) must be close to unity to achieve a complete utilization of the whole reactor volume. A second conclusion was that for a better performance, at a constant absorption coefficient, it is more convenient to employ catalysts having a minimum albedo ($\sigma/(\sigma+\kappa)$). The authors also made some experiments: they measured (with a UV radiation detector) the radiation flux coming out of the external surface of the annular reactor and compared these values with predictions from the Monte-Carlo simulation; the data were fitted reasonably well if a value of 0.5 was adopted for the TiO_2–water albedo.

Finally, among the different proposals for a heterogeneous photoreactor design based on theoretical analyses that model scattering, we can mention those methods that solve the RTE. According to the assumptions that are set forward one can obtain a mathematical (or numerical) problem of different complexity. The most evident simplification is to neglect scattering-in. Then, the problem looses its integro-differential mathematical structure.

Martín et al. [50–52] solved the RTE neglecting scattering-in under very restricted experimental conditions. They studied the photocatalytic decomposition of chloroform in aqueous solution employing polychromatic light. An annular reactor (Fig. 2) placed at the focal axis of a cylindrical reflector of elliptical cross-section was used; at the other focal axis a tubular UV lamp was located. Under very stringent geometrical limitations, this system permits fairly uniform irradiation of the reactor from outside. The reactor itself was constructed with three concentric cylinders: (i) the external annular space was used for keeping the reaction space at uniform and constant temperature; (ii) the intermediate annular space served two purposes: actinometric measurements (with uranyl oxalate) and photocatalytic reactions (substrate+water+catalyst) and (iii) the inner cylinder used also for actinometric measurements. Applying a parallel planes incident radiation model, the LVREA at any position (r) inside the reactor can be calculated from

$$e^{\mathrm{a}}(r) = \int_{\lambda} \mathrm{d}\lambda\, \kappa_{\lambda}{}^{*} C_{\mathrm{c}} \left\{ G_{\lambda,w,r_2} \left(\frac{r_2}{r}\right) \times \exp\left[-\beta_{\lambda}{}^{*} C_{\mathrm{c}} (r_2 - r)\right] \right\} \tag{7}$$

where $\kappa_{\lambda}{}^{*}$ and $\beta_{\lambda}{}^{*}$ are the specific (per unit mass) spectral absorption and extinction coefficients, respec-

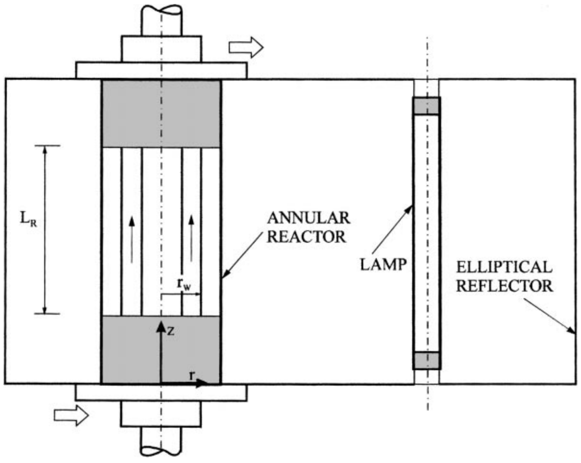

Fig. 2. Schematic representation of the annular photocatalytic reactor used by Martín et al. (adapted from Martín et al. [51,52]).

tively, r_2 the reactor external radius and G_{λ,w,r_2} is an experimentally measured boundary condition (with the actinometer in the intermediate annular space).

Using this method for calculating the LVREA the photocatalytic chloroform decomposition was studied; it was found that the quantum efficiency: (i) increases with increasing substrate concentration; (ii) is independent of the initial concentration of molecular oxygen provided that excess dioxygen is present and (iii) increases when the reactor volume averaged absorbed radiation decreases. The reaction kinetics were also investigated; it was found that the reaction rate is: (i) first order with respect to the substrate concentration; (ii) zero order with respect to the dioxygen concentration (molecular oxygen was always present in excess with respect to the stoichiometric demand) and (iii) order one half with respect to the reactor volume averaged LVREA.

Alfano et al. [53] studied scattering in a heterogeneous photochemical reactor; they used a flat plate reactor (Fig. 3). The experimental device was a continuous, perfectly mixed reactor inside the cycle of a batch system. It was illuminated with a tubular UV lamp and a parabolic reflector. The window for the radiation entrance was made of ground glass to produce diffuse emission. Inside the reactor a well-known homogeneous reaction (uranyl oxalate decomposition) produced the no-scattering condition; then, different concentrations of artificial scattering centers (inert, transparent silica beads or inert transparent latex spheres) were incorporated into the system giving rise to a change in the measured reaction rate for the homogeneous reaction.

A one-dimensional (x), one-directional (μ) mathematical model was used to evaluate the heterogeneous radiation field. Azimuthal symmetry was imposed on the irradiating condition of the experimental system (diffuse emission). In this way, the RTE can be reduced to the following form:

$$\mu\frac{\partial I_\lambda}{\partial X}+\beta_\lambda I_\lambda(x,\mu) = \frac{\sigma_\lambda}{2}\int_{\mu'=-1}^{1} I_\lambda(x,\mu')\,p(\mu,\mu')\,\mathrm{d}\mu' \tag{8a}$$

$$I_\lambda(0,\mu)=I_{0,\lambda},\quad (\mu>0) \tag{8b}$$

$$I_\lambda(L,\mu)=0,\quad (\mu<0) \tag{8c}$$

where $\mu=\cos\theta$. The discrete ordinate method was used to solve the RTE numerically. With the obtained values of intensities the LVREA was calculated according to

$$e_\lambda{}^{\mathrm{a}}(x)=\kappa_\lambda 2\pi\int_{\mu=-1}^{1} I_\lambda(x,\mu)\,\mathrm{d}\mu \tag{9}$$

This model was used by Cabrera et al. [54] to carry out a parametric study of scattering effects in a heterogeneous photoreactor. Among the different investigated variables three were more deeply analyzed: (i) concentration of transparent scattering centers; (ii) concentration of radiation absorption species and (iii) effects produced by the adoption of different phase functions. It was shown that in a perfectly

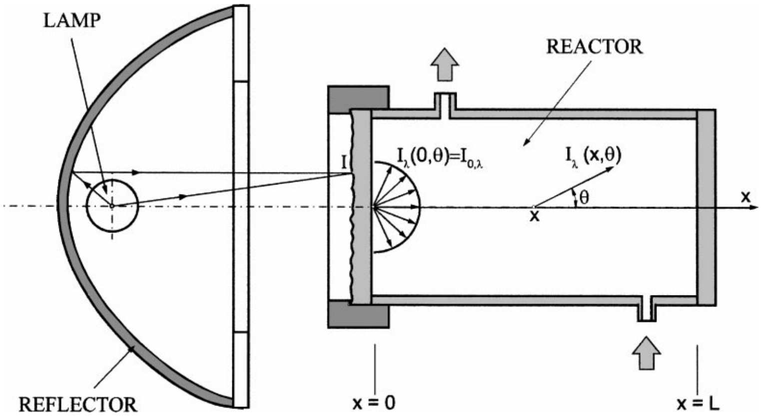

Fig. 3. Schematic representation of the unidimensional, flat plate photocatalytic reactor. (adapted from Alfano et al. [53]).

mixed photoreactor, increasing scattering always produces a decrease in the reaction yield. This effect is: (i) mild for a low absorbing medium; (ii) moderate for a highly absorbing medium and (iii) maximum for a system with moderate radiation absorption characteristics.

Using the same model and the same reactor, Alfano et al. [55] evaluated the LVREA for a photocatalytic system. They published a comparative study of different methods employed to evaluate the photon absorption rate (radiation flux at the wall of radiation entrance, homogeneous actinometry, solution of the RTE, etc.). They concluded that neglecting scattering would lead to significant errors. In particular, it will produce an important overestimation of the absorbed radiation.

Cabrera et al. [56,57] and Alfano et al. [58] used the same concepts to analyze experimentally overall quantum efficiencies in a heterogeneous photocatalytic reactor. The studied reaction was the TiO_2-catalyzed decomposition of trichloroethylene in water. With proper evaluation of the absorbed radiation energy (accounting for in- and out-scattering) the main conclusion was that in most situations scattering must be computed if serious underestimation of quantum efficiencies are to be avoided. A key point in obtaining these results was the development of special experimental techniques to obtain separate values for specific (per unit mass) absorption and scattering coefficients as a function of wavelength [27].

Along the same lines of work, Brandi et al. [59,60] made a significant improvement in the method. They managed to release the model from the restriction of working with devices having azimuthal symmetry in the irradiating condition. The new model was a two-dimensional (x, y), two-directional (θ, ϕ) representation. It was applied to a bench scale, flat plate, continuous photocatalytic reactor irradiated with two tubular UV lamps and two parabolic reflectors; this system emulated a solar collector having an almost constant radiation flux at the reactor wall facing the lamps. The appropriate mathematical solution were obtained employing the DOM. For two different titanium dioxide photocatalysts (Aldrich and Degussa P25) the model permitted the proper evaluation of LVREA profiles inside the reactor. From the radiation point of view, and for a reactor having a thickness of 1 cm, the optimal catalyst concentration was about 0.5 g/l.

Finally, just recently, Romero et al. [61] solved the RTE for a cylindrical geometry. They studied an annular reactor having a lamp at its centerline. Different scattering centers were used (transparent silica beads, transparent latex spherical particles and Aldrich and Degussa P25 TiO_2 catalysts). The employed model was a two-dimensional (r, z), two-directional (θ, ϕ) representation of the radiation field. Emission by the lamp — with no restrictions — was described with the extended source, voluminal emission model [26].

Radiation profiles along the r and the z coordinates were found to be highly non-uniform. The last observation (z-direction) is the result of using a lamp having the same length as the reactor length. Conclusions about an optimal catalyst concentration — from the radiation point of view — coincide with those reported by Brandi et al. [59] for the flat plate reactor.

2.2. Experimental design

The experimental design approach is a methodology quite different from those described previously. Recognizing that too many parameters affect the performance of a photocatalytic reactor, particularly with substrates of complex composition, an experimental approximation that can be useful to orient future laboratory work and even the design of actual applications was devised. In these cases, usually the photon absorption rate is only implicitly included in the design methodology.

Three unrelated methods have been used in photocatalytic reactors (Table 2): (i) one based on the well-established optimal experimental design; (ii) the second is based on artificial neural networks and (iii) the third is based on an empirical approximation. Jakob et al. [62] and Braun et al. [1] applied the ideas of optimal experimental design to analyze the performance of an immersed multi-lamp photochemical reactor. The authors proposed to carry out carefully selected experiments in order to obtain the best operating conditions for a given reaction and with a pre-established objective. They applied these ideas to the photocatalytic decomposition of a mixture of different organic compounds (mainly nitroaromatics resulting from industrial wastewater) using TiO_2 as a catalyst. Based on the previous knowledge of the complex-system chemistry five variables were selected: initial TOC concentration, wastewater flow rate into the reactor, provision of an electron acceptor (air or pure molecular oxygen), catalyst concentration and temperature. After application of a factorial design (2^3), the authors generated a three-dimensional representation of the reaction rate as a function of the initial TOC and catalyst concentration at different constant temperatures. They concluded that the maximum reaction rate could be obtained working at 80°C with 5 g/l of catalyst and an initial TOC of 4500 ppm.

Artificial neural networks constitutes a different method for the same type of objective. This technique does not require the previous knowledge of a mathematical representation of the process performance and it has the ability to "learn and record" the system behavior (linear or non-linear responses with respect to the operating variables) from the information provided by a set of experimental data.

This method was used by Braun et al. [1] to analyze a well-known photochemical reaction: the photodecomposition of uranyl oxalate. The reaction space (an annular, continuous reactor) was placed at one of the foci of an elliptical reflector. The following variables were selected: flow rate, reactor inner diameter and reactor length (or reactor volume). After several experimental runs, the "learning step" by the neural network was completed and the reactor performance could be simulated. Then the authors made a scale-up of the system. Afterwards they compared the experimental data from the larger size reactor with predictions obtained with the neural network simulator. Conversion vs. flow rate results yielded good agreement.

Jakob et al. [62] used artificial neural networks to study the degradation of the same complex organic mixture quoted above (wastewater in an immersed multi-lamp reactor).

After the learning procedure with experiments, the authors produced a set of predictions with the simulator. Data of reaction rates vs. catalyst concentration indicated that 2 g/l of titanium dioxide rendered the optimum performance (although a plateau from 2 to 10 g/l observed). With a response surface obtained from simulation results, the following conditions for optimal degradation rates were obtained: 80°C, 2 g/l of TiO_2 and 5000 ppm for the TOC.

A third approach based on an empirical approximation was used by Ray and Beenackers [63], Ray [64] and Mukherjee and Ray [65] to analyze different reactor configurations in order to improve light distribution inside the reactor space. The authors proposed the use of a "reactor specific parameter" (κ that represents the illuminated catalyst surface area in contact with the reaction liquid inside the reactor volume ($\mathrm{m^2\,m^{-3}}$)) and a "reaction specific parameter" ($\mathfrak{R}$, representing the average mass destruction rate ($\mathrm{mol\,m^{-2}\,s^{-1}}$)) to discuss the different reactor performances.

In order to complete this partial review, we are including here a contribution to photoreactor analysis that does not fall into the previous categories but deserves mention related to the proposal of a new type of thin-film reactor and its approximate mathematical model. In this proposal the volume of a thin slurry of the solid suspension is bounded by one wall of a cylindrical reactor. A falling film descends along the internal side of this column and is irradiated by a lamp axially mounted in the middle. This design is particularly good for avoiding the well-known problem of reactor wall fouling by titanium dioxide, the model has been validated with experiments published in a second paper by the same authors [66,67].

3. Solar photocatalytic reactors for wastewater treatment plants

3.1. Main issues

Several comprehensive articles have been published during the last years discussing the design of solar photocatalytic reactors and solar wastewater treatment plants [68–71]. It seems therefore appropriate to concentrate our effort on the most important topics concerning their applications.

Two of the major design issues for solar photoreactor systems are: (i) whether to use a suspended or a supported photocatalyst and (ii) whether to use concentrated or non-concentrated sunlight.

Until now, the majority of tests of solar photocatalytic reactors and treatment plants have been using small particles of the photocatalyst (usually titanium dioxide) suspended in the contaminated water. The main advantages of these slurry systems are: (1) low pressure drop through the reactor; (2) better availability of the catalytic surface area for adsorption and reaction and (3) good mass transfer of the wastewater contaminants from the fluid to the photocatalyst. The major disadvantage of systems containing suspended solids is the need to remove the photocatalyst from the cleaned water after the treatment. Most of the titanium dioxide powders used in photocatalysis contain submicron-sized particles. As a consequence, the potential inexpensive separation by sedimentation or filtration of the suspension is troublesome and treating very large volumes of water is almost impossible. Systems using a supported photocatalyst eliminate the need for a catalyst separation step. However, it has been frequently reported that the process efficiency is reduced when the catalyst is fixed [72–75] and it has recently been shown that for the same catalyst loading slurry reactors are more effective than fixed-bed systems [76].

Light concentrating systems in which the solar light is concentrated in a photocatalytic reactor by a reflecting surface have the important advantage that, for the same light harvesting area, the reactor volume may be smaller than in a non-concentrating system. This allows the use of more expensive components for the reactor without adversely affecting the overall cost. In general, stronger reactors, which are able to withstand higher pressures and possess the possibility of employing costly supported catalysts, can be built. Moreover, they can be operated at much higher flow rates improving mass transfer rates.

On the other hand, non-concentrating (“one sun”) systems have other advantages: (1) The lack of a reflective surface reduces optical losses. (2) One-sun systems can use more sunlight as they are able to capture the diffuse UV light as well as direct solar beams. The diffuse component can make up to 50% of the total available UV light even on a clear day because the shorter wavelengths UV photons are more readily scattered within the atmosphere. Additionally, under cloudy conditions, only the diffuse solar UV light is available, and — unlike a focusing system — a non-concentrating system can continue its operation. (3) One-sun reactors are able to use the light more efficiently than concentrating systems. This is supported by experimental results which show that the efficiency of most photocatalytic processes decreases as the UV energy flux density increases [4,5].

Although one-sun systems possess important advantages when compared with light concentrating systems, there are also some disadvantages: (1) The reactor in a non-concentrating system is usually much larger than in a concentrating one because the photoreactor in a one-sun system is both the solar collector and the photocatalytic reactor. (2) A non-concentrating photoreactor requires a large area of weather resistant, chemically inert, UV-transmitting glazing when a containment of volatile wastewater pollutants is necessary. Such a large surface necessitates the use of relatively inexpensive building material for this containment. (3) The materials which best meet these requirements are certain types of plastics. However, most plastic materials possess lower tensile strength than the rigid glass pipes used in concentrating reactors, thus reducing the pressure capability of the photoreactor system. This combination of pressure limitations, large volume demand, need to keep the photocatalyst suspended, and requirement of high fluid to solid mass transfer rates enforces a careful design of the reactor’s hydrodynamics and of the respective flow control.

A solar wastewater treatment facility may be operated either in a continuous and single-pass mode (once through) or in a batch mode. In the single-pass mode (Fig. 4a) the irradiated reactor area and the flow rates have to be designed ensuring that the desired destruction of the water contaminants is achieved in a single-pass. Since the solar flux density varies throughout the day, the flow rate through the solar reactor must therefore be varied following the flux density of the solar energy. As the UV flux density decreases, the flow rate through the solar reactor must be decreased (alternatively, the number of reactors has to be increased, an economically unacceptable solution) in order to maintain the same final concentration of the pollutants in the treated wastewater. On the other hand, in the discontinuous batch mode (Fig. 4b) the wastewater is stored in a tank and continuously recirculated through the solar reactor until the desired final concentration of the pollutants is achieved. However, this operating form —as typical of batch processes— sets restrictions to the flexibility of the volume of wastewater which can be treated. Up to now most solar photocatalytic wastewater treatment plants have been operated in the batch mode.

3.2. Reactors for solar photocatalytic wastewater treatment

As mentioned above, the major design issues for solar photoreactor systems are whether to use a sus-

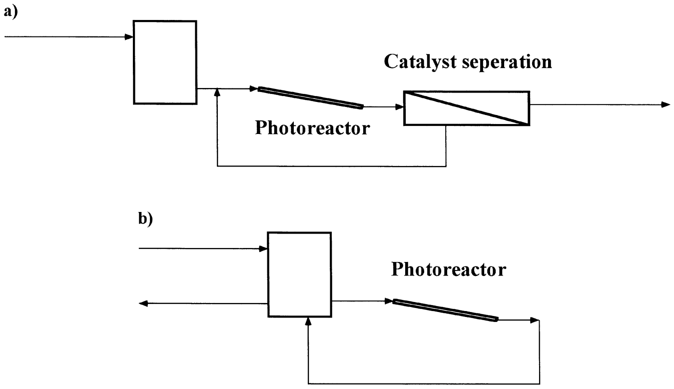

Fig. 4. Schematic representation of design concepts for solar wastewater treatment plants: (a) a once-through reactor and (b) batch operation.

pended or a supported catalyst and whether to use concentrated or non-concentrated sunlight. Consequently, very different reactors for the solar photocatalytic water treatment have been developed and tested in recent years. They are summarized in Table 3.

The reactors most often used are (1) parabolic trough reactors (PTRs); (2) compound parabolic collecting reactors (CPCRs); (3) other tubular reactors with and without reflectors; (4) the double-skin sheet reactor (DSSR) and (5) the thin-film fixed-bed reactor (TFFBR). These reactor types will be described in more detail below.

A parabolic trough reactor consists of a reaction pipe and a light reflecting trough and can be characterized as a typical tubular reactor that could be operated in the plug flow mode. The reflector has a parabolic profile with the reaction pipe in its focal line (Fig. 5a). Consequently, only direct radiation entering the parabolic trough normal (or almost normal) to its aperture can be focused into the reaction pipe and a one or two-axis sun-tracking system is required. A PTR concentrates the direct rays of the photocatalytically active UV part of the solar spectrum by a factor of 20–50. It should be noted that under air mass 1.5 conditions, the diffuse ($E_{\mathrm{dif}(300\text{–}400\,\mathrm{nm})}=24.3\,\mathrm{W cm}^{-2}$) and direct ($E_{\mathrm{dir}(300\text{–}400\,\mathrm{nm})}=25.0\,\mathrm{W cm}^{-2}$) portion of the solar radiation reaching the surface of the earth are almost equal [93]. This means that a light concentrating system can, in principle, only employ half of the solar radiation available in this particular spectral region.

Table 3
Preponderant types of solar reactors

Light-concentrating properties	Photocatalyst	
	Suspended	Supported
Concentrating reactors	Parabolic trough reactor [70,77–81] Falling film reactor [77,78]	Parabolic trough reactor [70]
Non-concentrating reactors with reflector	Compound parabolic collecting reactor [70,80,81]	Tubular reactor [82] Fiber optic cable reactor [83]
Non-concentrating reactors without reflector	Solar pond [81,84,85] Tubular reactors Inflatable tube reactor [71] Pressurized tube reactor [70,86] Flat plate reactors Trickle-down flat plate reactor [87] Double-skin sheet reactor [88,89] Falling film reactor [71]	Flat plate reactor Trickle-down flat plate reactor [87] Thin-film fixed-bed reactor [90–92]

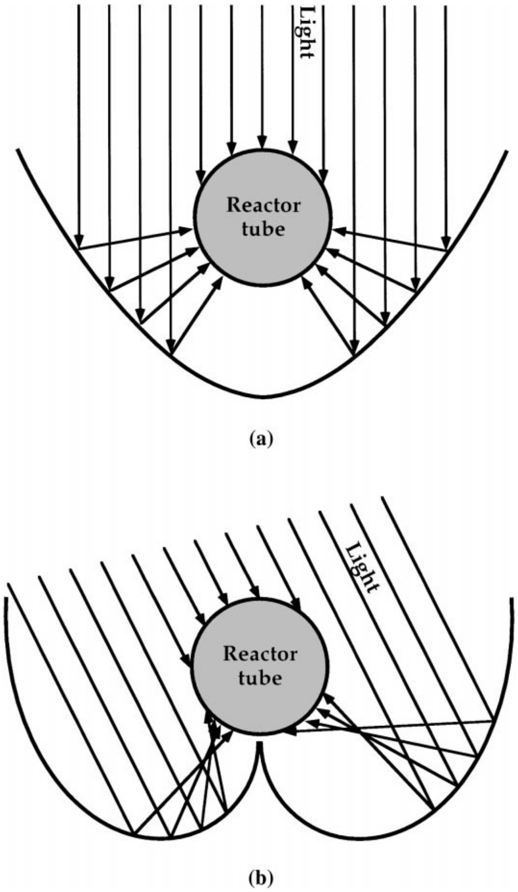

Fig. 5. Geometric profile of: (a) a Parabolic trough reactor (PTR) and (b) a compound parabolic collecting reactor.

Parabolic trough reactor types have been chosen for solar detoxification loops constructed in Colorado, USA (by National Renewable Energy Laboratory, NREL and subcontractors), in Albuquerque, USA (by Sandia National Laboratories), in California, USA (by Lawrence Livermoore National Laboratories) and in Almeria, Spain (by the Plataforma Solar de Almeria, PSA) [70,79–81,94–105]. While in the USA mainly single-axis tracking parabolic trough reactors were used, at the PSA a reactor with a two-axis tracking trough has been installed.

A typical single-axis tracking PTR was developed by Industrial Solar Technology, Denver, CO, USA. This system consisted of 6.1 m long by 2.1 m wide parabolic trough collectors with a 5.1 cm diameter borosilicate glass receiver tube. The surface of the troughs was covered with a reflective polymer film (laminated onto an aluminum back sheet) designed to enhance reflection of UV light. The UV reflectivity of this film was approximately 85%. The effective concentration ratio, including optical losses, was approximately 20 [69]. Usually titanium dioxide slurries were used with this reactor type, but this trough system was also used to test the performance of two different supported photocatalysts (titania coated on a stainless steel screen, which was folded into a tubular accordion shape, and titania bonded onto fiberglass strands) [69]. Another type of PTR, which is controlled by a two-axial (azimuth and elevation) tracking system, has been developed from the heliostat “Helioman” built by MAN, Germany, (Fig. 6) [79]. Here the solar rays are concentrated by parabolic trough mirrors (aperture area: 32 m^2) with an aluminized UV-reflective surface and focused on borosilicate glass tubes, which are filled with the contaminated aqueous TiO_2-suspensions. Due to losses caused by reflectivity, translucence and system errors the yield of the UV light photons reaching the contaminated suspensions is about 58% of the original light intensity entering the aperture plane of the heliostat.

A CPCR is a trough reactor without light concentrating properties. It differs from a conventional PTR by the shape of its reflecting mirrors. The shape of a CPCR reflector usually consists of two half cylinders of parabolic profiles set side by side. The center line (equivalent to a focal axis) is located closely above the connection of the two parabolic profiles (Fig. 5b). This geometry enables light entering from almost any direction to be reflected into the “focal” line of the CPCR, i.e., most of the diffuse light entering the module can also be employed for the photocatalytic reaction. Due to this geometry a CPCR must not track the sun but exhibits only a small concentration factor (<1.2). The azimuth of the CPCR should be adjusted to the complementary angle of the geographical altitude and the pipes should be aligned south and from top to bottom. As an example a schematic view on a CPCR manufactured by Industrial Solar Technology is given in Fig. 7, while Fig. 8 shows a photograph of this CPCR installed at the PSA. This type of reactor has been tested at the out-door test field of NREL in USA [69] and at the PSA in Spain [80,81,101,102,106–111].

The CPCRs at the PSA have a concentration factor of 1.15, i.e., this type of reactor has practically

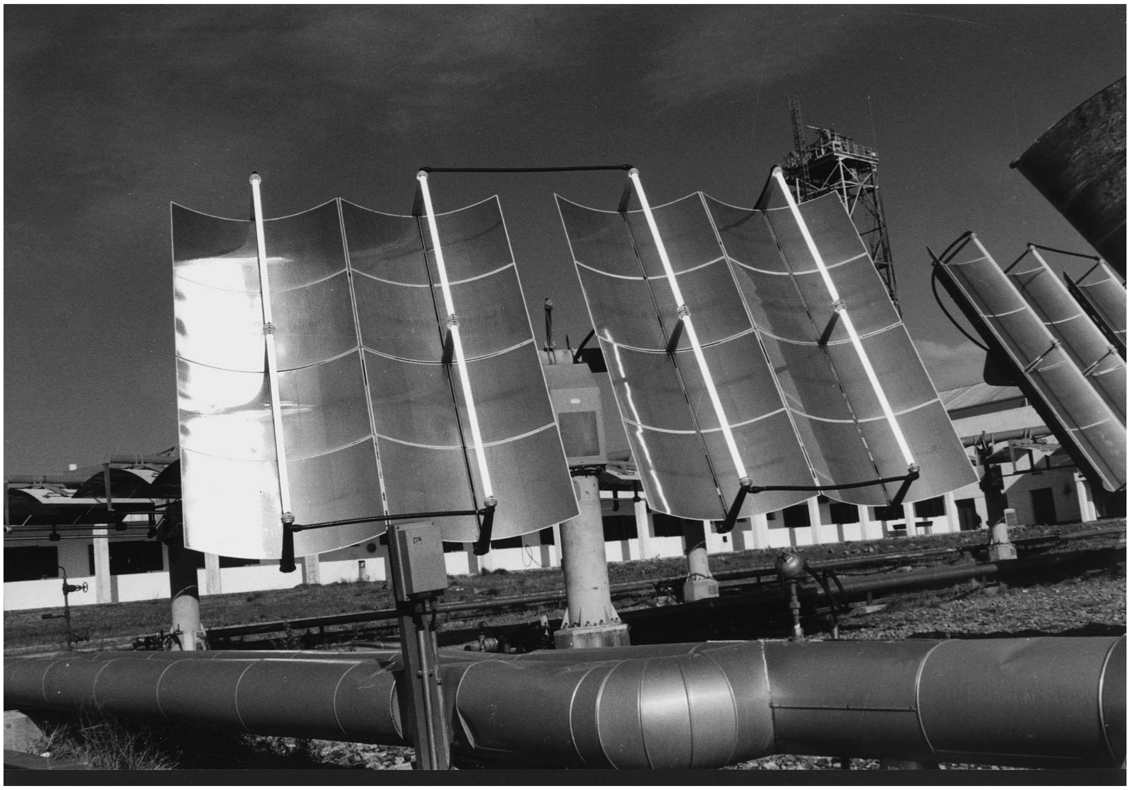

Fig. 6. View of a parabolic trough reactor, type “Helioman”, installed at the PSA (Photo: Goslich).

no light concentrating properties (*vide supra*). One CPCR-module consists of eight parallel reflectors made from polished aluminum. This material has very good reflection properties especially in the UV region of the solar spectrum. In the spectral range of 295–387 nm its reflection efficiency is 83.2%. A single CPCR reflector has a length of 1.22 m and a width of 0.152 m, i.e., the effective light harvesting area of one module consisting of eight reflectors adds up to 1.48 m^2. A reaction pipe made of a transparent fluo-

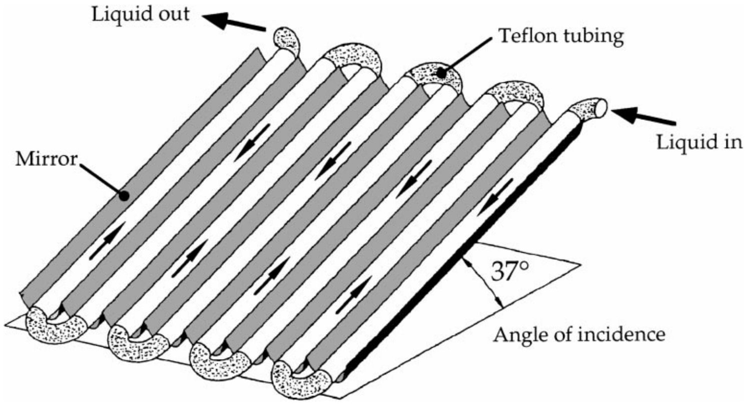

Fig. 7. Schematic representation of a single CPCR module installed at the PSA.

Fig. 8. View of compound parabolic trough reactors installed at the PSA (Photo: Goslich).

ropolymer (Teflon) is fixed in the "focal" line of each CPCR reflector through which the suspension containing the photocatalyst and the pollutant circulates. The transmissivity of Teflon in the spectral range under consideration is 76.8%, thus limiting the theoretical reactor efficiency to 63.9%. The absorber pipe is as long as the module (1.22 m), has an inner diameter of 48 mm and consequently an illuminated volume of 2.21 l per pipe. The cylindrical reactor surface area for eight tubes is 1.47 m^2. The connectors between the absorber pipes consist of polypropylene pipes.

One-sun tubular reactors with a reflector and packed with a supported photocatalyst were recently introduced by Crittenden et al. [82,112,113] and tested at Tyndall Air Force Base, Florida, USA at a fuel contaminated site. The photoreactors were constructed in a series of plastic tube segments made from M-7® plastic (American Energy Technologies, Green Cove Springs, Florida, USA). The inner diameters of the reactor tubes were 0.64 or 1.27 cm, respectively. The wall thickness of the reactors was 0.16 cm. The averaged sunlight transmittance of 0.32 cm thick M-7® material was greater than 80% in the wavelength range 300–400 nm. The reactors were packed with a silica-supported titanium dioxide photocatalyst (Aldrich TiO_2 on Aldrich 35×60 mesh Davisil™ silica gel). The bed porosity of the packed reactor was 0.39. Up to four reactors were mounted in front of a flat plate metal reflector, 15 cm apart from each other, and 8 cm removed from the reflector. The flat metal plate reflected approximately 80% of the UV portion of the solar radiation. The plate was placed facing the south tilted approximately 30° from the horizontal to maximize solar insolation.

A one-sun tubular reactor (SOLTOX™) without reflector was developed by American Energy Technologies in conjunction with the University of Florida and installed for field testing at the same site at Tyndall Air Force Base [69,86,114,115].

This reactor consists of a bank of transparent tubes (0.64 cm inside diameter) with a length of 2.4 m. Sixty-six of these tubes run from a CPCR header to a similar downstream CPCR manifold (each with 3.8 cm inner diameter) giving a total aperture area of 1.0 m^2 per sub-module. Two such sub-modules were linked together with pipes to form a photoreactor module.

A new kind of a non-concentrating flat plate reactor is the double-skin sheet reactor (DSSR) which has been developed by Röhm GmbH Chemische Fabrik, Darmstadt, Germany and the Institut fuer Solarenergieforschung GmbH, Hannover, Germany (ISFH). The DSSR consists of a modified double-skin sheet (SDP 16/32) manufactured by the Röhm GmbH in Darmstadt, Germany which is now commercially available (Solacryl Gesellschaft für Regenerative Energiesysteme mbH, Elsenfeld, Germany). PLEXIGLAS® (polymethyl methacrylate) is used to produce the flat and structured box of the photoreactor [88,89]. The comparison of the spectral irradiance of the sun with the transmission spectrum of the plastic used to manufacture the double-skin sheets evinces that the UV-A portion of the solar spectrum below 400 nm nicely matches with the onset of the PLEXIGLAS®-transmission [89]. Typically one module has a length up to 2.50 m, a width of 0.98 m and contains 30 interconnected rectangular-shaped channels (2.85 cm × 1.2 cm). The inner structure of the reactor is schematically drawn in Fig. 9. The suspension containing the polluted water together with the photocatalyst is meandering through these channels. Independently from the ISFH group, a similar reactor has been developed at the University of Florida [71,116].

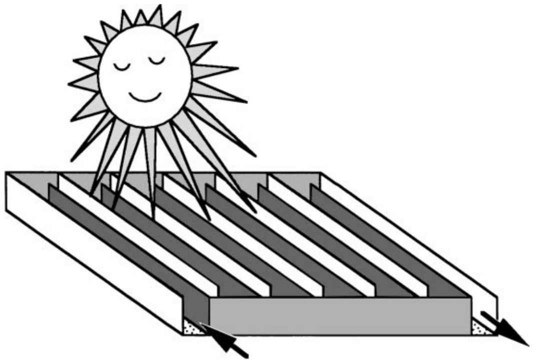

Fig. 9. Schematic representation of the inner layout of a DSSR.

One of the first solar reactors using a fixed photocatalyst and not applying a light-concentrating system for the photocatalytic process is the thin-film fixed-bed reactor (TFFBR), depicted in Fig. 10 [90,104]. The most important part of the TFFBR is a sloping glass plate (width 0.60 m × height 1.20 m) coated with the photocatalyst (e.g., titanium dioxide Degussa P25 or Sachtleben Hombikat UV100 [117]). The polluted water flows along the inclined glass pane forming a very thin film (~100 μm).

3.3. Comparison of different solar reactors

Extensive degradation experiments have been performed at the PSA in Almeria to compare the efficiencies of the PTR (heliostat) and the TFFBR [90,104,105], e.g., the complete stoichiometric degradation of the model pollutant dichloroacetate (DCA) was observed in both types of reactors and in agreement with laboratory results. The rate of the DCA-degradation was found to exhibit a linear dependency on the light intensity at pH~3 [90]. Since the TFFBR is able to use also the diffuse part of the UV sunlight, its photocatalytic activity could even be observed on very cloudy days with almost no direct solar radiation. Moreover, within an initial DCA-concentration range between 1 and 5 mmol l^{-1} the TFFBR always reached a higher degree of degradation than the parabolic trough reactor. For an initial DCA-concentration of 1 mmol l^{-1}, nearly 100% conversion could be achieved in a single path experiment using the TFFBR [104]. It became apparent from the comparison of these reactor types that it is a major engineering problem of the PTR to maintain a sufficient concentration of molecular oxygen throughout the reactor. Using small flow rates to assure high residence times resulted in an accumulation of oxygen bubbles in the tubes thus reducing the illuminated volume and lowering the degradation rates. Since electron scavengers such as H_2O_2 can be dissolved in water without the formation of bubbles, an enhanced DCA-degradation was observed in the presence of H_2O_2 when molecular oxygen was absent [90,104,105].

As an example of a real wastewater stream the degradation of industrial wastewater from a phenolic

Fig. 10. View on a TFFBR (Photo: Goslich).

resin factory has been investigated with both types of reactors [100,103,104]. These experiments were performed in a closed loop simultaneously with both reactor types to ensure identical solar illumination intensities. While only 30% of the relative initial total organic carbon concentration ((TOC)/(TOC)^0) were degraded after 250 min using the PTR, a decomposition of more than 70% was obtained after the same time with the TFFBR [90,103,104]. However, it must be noted that in the case of the film reactor the authors observed a considerable decrease of the TOC concentration without illumination which was explained by the vaporization of volatile components from the effluent water. This is a general problem of all open reactor systems due to the ready equilibration with the surrounding atmosphere. Encapsulation of the reactor presents a feasible yet rather costly means to overcome this disadvantage. However, in particular when gas injection units are used to ensure a sufficient concentration of molecular oxygen in the wastewater stream, a partial volatilization of pollutant molecules with high vapor pressure can hardly be prevented and must be solved, e.g., by separate waste gas purification systems. Nevertheless, this comparative study evinced that it is possible to achieve good photocatalytic detoxification efficiencies without using light concentrating solar reactors. Furthermore, the TFFBR offers the advantages of a less expensive construction and, when the catalyst is properly fixed, reduced running costs as compared with the PTR. Also the fixation of the ultrafine photocatalyst particles solves the complex problem of the otherwise needed filtration unit for the separation of the catalyst from the purified wastewater.

Recently Malato Rodríguez et al. [80] have compared the PTR installed at the PSA with a CPCR using real wastewater obtained from a chemical company specializing in the synthesis of phenolic resins and a distillation residue from a pharmaceutical company, respectively. Degussa P 25 was used as the photocatalyst and peroxydisulfate as an additional oxidant. In comparison with the PTR, the CPCR always exhibited the better performance.

Moreover, Richter et al. [102] reported their results of a comparison between a concentrating and a non-concentrating solar reactor performing simultaneous degradation experiments employing dichloroacetic acid as the model pollutant. The concentrating system was a two-axis sun-tracking PTR (Helioman) with an overall aperture area of 29.1 m^2 and an irradiated volume of 44 l. The non-concentrating system consisted of six CPCRs with an overall aperture area of 9 m^2 and an irradiated volume of 110 l. The CPCRs were fixed and tilted at an inclination of 37°. The performances of these systems were compared by calculating the overall organic carbon degradation rate per collector aperture area (mg carbon $\mathrm{m}^{-2}\,\mathrm{h}^{-1}$) during the initial phase of the simultaneous experiments. The CPCRs showed a performance in the range 300–600 mg carbon $\mathrm{m}^{-2}\,\mathrm{h}^{-1}$, approximately fivefold higher than that of the PTRs [102].

To quantify the influence of the applied irradiation on an experiment it is necessary to correctly evaluate the amount of radiation that has been absorbed by the suspension at any specific time of the experiment as well as the corresponding changes in the concentration of the pollutants. In many practical applications the mass of the organic pollutants contained in the treatment plant at any specific time is often determined by recording the TOC content of the water in regular time intervals and multiplying this value by the overall volume of the suspension, V_t. The solar light energy is usually applied to a limited surface area, namely the aperture of the PTR or the CPCR, the glass pane of the TFFBR or the PLEXIGLAS® sheets of the DSSR, respectively. To account for these differences the so-called “mass area ratio” S_TOC of the organic pollutant has recently been proposed by Goslich et al. [109]. This has been defined as the overall mass of the pollutant degraded per unit surface area of the reactor, A_r

$$S_\mathrm{TOC} = \frac{\mathrm{TOC} \times V_\mathrm{t}}{A_\mathrm{t}} \tag{10}$$

The change of S_TOC with time ($\mathrm{d}S_\mathrm{TOC}/\mathrm{d}t$) yields the effective degradation rate for a specific reactor, R_eff, where dt can be replaced by the effective experimental time t_exp provided that the degradation rate is found to be reasonably constant over the duration of the experiment

$$R_\mathrm{eff} = \frac{\mathrm{d}S_\mathrm{TOC}}{\mathrm{d}t} \approx \frac{\Delta S_\mathrm{TOC}}{\Delta t_\mathrm{exp}} \sim \frac{S_\mathrm{TOC}}{t_\mathrm{exp}} \tag{11}$$

i.e., R_eff specifies the degraded mass per unit time interval and per unit surface area of the irradiated reactor. This mass area ratio will be strongly dependent on the incident light energy, i.e., it will depend on the illumination time. To account for the fluctuations of the spectral solar irradiance with time it is reasonable to divide the mass area ratio of the pollutant S_TOC by the total UV radiation, $E_\mathrm{UV,tot}$, accumulated at a specific time of the experiment yielding the “efficiency”, η, of the reactor under consideration [109]

$$\eta = \frac{S_\mathrm{TOC}}{E_\mathrm{UV,tot}} \tag{12}$$

This efficiency η relates the degraded mass of the pollutant to the irradiation energy reaching the reactor surface and hence represents a lower limit for the efficiency of a reactor, as it does not take into account any losses of the photon energy due to reflection, scattering, absorption in reactor walls, etc. The efficiency η is comparable to the apparent photonic efficiency ζ

with the difference that ζ has the dimensions of mol (of degraded compound) per Einstein, whereas η has the dimensions of mass (of degraded compound) per unit of accumulated energy arriving at the reactor. The determination of η seems to be particularly useful in the case of fluctuating radiation conditions, e.g., for solar reactors. Recently, Goslich et al. [109] have determined η for the photocatalytic degradation of the model pollutant dichloroacetate, DCA, at different catalyst concentrations to compare the efficiencies of the CPCR and the DSSR under identical solar illumination conditions at the PSA. The reactor efficiency for the degradation of DCA in the presence of Degussa P25 was found to range from about $1.0\,\mu\mathrm{g\,J^{-1}}$ at the lowest catalyst concentrations employed ($0.25\,\mathrm{g\,l^{-1}}$) to about $3.0\,\mu\mathrm{g\,J^{-1}}$ at a catalyst concentration of $1\,\mathrm{g\,l^{-1}}$. The increase in efficiency above $1\,\mathrm{g\,l^{-1}}$ was found to be much slower; in the CPCR η even decreased to about $2.5\,\mu\mathrm{g\,J^{-1}}$ at a catalyst concentration of $5\,\mathrm{g\,l^{-1}}$ P25. This behavior is similar to that observed in laboratory experiments [118]. It was therefore concluded that it is not necessary to use catalyst concentrations exceeding $1\,\mathrm{g\,l^{-1}}$ to sufficiently degrade this model pollutant when P25 is employed [109]. Furthermore, the authors pointed out that laboratory experiments could be used as an “order of magnitude” approximation for the behavior of real pilot installations. The same effect was observed using Sachtleben Hombikat UV100 as the photocatalyst [109].

The comparison of the results obtained on the pilot plant scale [109] with recent laboratory data evinces that a plot of the reactor efficiency η as a function of the catalyst concentration yields a similar shape as that of the photonic efficiency ζ determined in laboratory experiments [118]. This qualitative similarity is a good indication for the ease and usefulness of the definition of η. Moreover, when the concentration of the organic pollutants is monitored by a TOC measurement the reactor efficiency η can be converted into the photonic efficiency ζ via [109]

$$\zeta = 28.01\eta \tag{13}$$

provided that η is given in $\mathrm{mg\,TOC\,J^{-1}}$. The conversion factor has the dimension of $\mathrm{J\,mg^{-1}}$, considering that all photons entering the reactor have an average energy of 5.6×10^{-19} J (assuming a mean illumination wavelength of 355 nm) and establishes the relation between this energy and the mass of a carbon atom (2.0×10^{-20} mg). This conversion leads to an apparent photonic efficiency ζ of 5.1% for the degradation of dichloroacetate employing P25 at a catalyst concentration of $0.25\,\mathrm{g\,l^{-1}}$ and of 11.7% for Hombikat UV100 at identical concentration, both values measured in the CPCR [109]. These values are also quantitatively almost identical to those obtained in laboratory experiments using 50 ml reactors and artificial illumination [118].

It is a surprising result of the study by Goslich et al. [109] that the reactor efficiencies obtained from the experiments performed in the DSSR are always slightly better than those measured in the CPCR since no special efforts had been made to optimize the overall reactor concept of the DSSR [89]. The CPCR, on the other hand, presents a reactor design in which efforts have been especially made to optimize the collection of diffuse and direct sunlight.

3.4. Solar photocatalytic treatment of contaminated water

Despite its obvious potential for the detoxification of polluted water, there has been very little commercial or industrial use of photocatalysis as a technology so far. The published literature shows only a few engineering scale demonstrations for the solar photocatalytic treatment of polluted groundwater, landfill leachates, and industrial wastewater in USA and in Europe. First engineering scale field experiments have been conducted in 1991 by the National Renewable Energy Laboratory (NREL) and the Sandia National Laboratories at a California Superfund Site located at Lawrence Livermoore National Laboratory (LLNL) treating ground water contaminated with chlorinated solvents, mainly trichloroethylene (TCE) [95–97]. This field system comprised of two drive strings of commercially available single-axis tracking parabolic trough reactors (Solar Kinetics). The reflective surfaces of the collectors consisted of a highly reflective aluminized film (SA-85, manufactured by 3 M). Each drive string was 36.5 m long and 2.1 m wide. The total aperture area of the pilot plant was $155\,\mathrm{m^2}$. The troughs were aligned on an east–west axis and controlled to automatically track the sun. The reactor consisted of a 5.1 cm internal diameter borosilicate glass pipe. The effective concentration ratio of this configuration, including reflective and transmissive losses, was calculated to be approximately 20. Prior laboratory tests had shown that the reaction rate was lowered by the high bicarbonate concentration of the groundwater under investigation (500 ppm). Therefore, tests were performed with and without the addition of acid to the contaminated groundwater. The flow rate was adjustable between 15 and 114 $\mathrm{l\,min^{-1}}$. The system was operated either in a once through (single-pass) or in a batch mode. Water from the polluted aquifer was pumped out of monitoring wells into a 570 l tank. In single-pass runs, the water from the tank was mixed with a slurry containing the TiO_2 catalyst (Degussa P25), passed through the PTR and reached the settling tanks directly where the catalyst was removed [95–97]. When the system was operated in the batch mode, the water was pumped from the tank through the PTR and back into the same tank. In single-pass runs the flow rate was held at approximately 15 $\mathrm{l\,min^{-1}}$ resulting in a residence time of 10 min. A TiO_2 slurry metering pump provided a catalyst loading of approximately 0.8 to 0.9 $\mathrm{g\,l^{-1}}$ (Degussa P25). With this relatively low titanium dioxide content, the TCE concentration was reduced from 107 to 10 ppb at pH 7.2 and from 106 to less than 0.5 ppb at pH 5.6 [95,97]. Batch experiments were performed varying the flow rate, the pH, the catalyst loading and the solar UV energy flux density. The data from these experiments showed that solar photocatalytic water treatment can reduce trichloroethylene in groundwater to levels below those required to meet drinking water standards [97]. The major conclusions from the batch experiments were: (1) the reaction kinetics are strongly dependent on the pH, with higher rates obtained at lower pH; (2) the reaction rates are weakly dependent on the catalyst loading in the range 0.3–1.0 $\mathrm{g\,l^{-1}}$ and (3) the reaction rates are independent of the flow rate [96,97]. By positioning the PTR horizontally (pointed straight up) the system was operated under one-sun conditions. It was observed that this configuration was roughly eight times more efficient than the concentrating configuration when the experimental results were normalized to the light harvesting area [97].

Parallel to the work performed in USA under the direction of NREL and Sandia National Laboratories, several research groups from different European countries, funded by the European Community, have tested the solar detoxification loop with its parabolic trough reactors installed at the PSA (Spain) since 1991.

Fig. 11 shows a schematic flowsheet of the installation at the PSA [79]. The PTR detoxification loop consists of 12 parabolic trough modules (type “Helioman”, MAN) connected in series and controlled by a two-axial tracking system. The solar rays are concentrated by parabolic trough mirrors (total aperture area: 384 $\mathrm{m^2}$) with an aluminized UV-reflective surface and focused on borosilicate glass tubes [79] which are filled with the contaminated aqueous TiO_2-suspensions moving at flow rates between 250 and 3500 $\mathrm{l\,h^{-1}}$ The total loop volume is 838 l. Research with this large experimental plant initially focused on the destruction of single compounds and mixtures prepared on-site [90,98,99,102–111] but recently the loop has also been used for the treatment of real wastewaters. Using the PSA detoxification loop, Blanco and Malato [99] conducted an engineering scale field demonstration of the treatment of industrial wastewater from a resins factory. This effluent contained organic contaminants such as phenol, phthalic acid, fumaric acid, maleic acid, glycols, xylene, toluene, methanol, butanol and phenylethylene amounting to a total of 600 ppm TOC. Employing 0.1 $\mathrm{g\,l^{-1}}$ Degussa P25 as the photocatalyst and 7 $\mathrm{mmol\,l^{-1}}$ sodium peroxydisulfate ($Na_2S_2O_8$) as the additional oxidizing agent besides molecular oxygen, the authors observed a complete TOC degradation within 44 min of illumination of a dilute solution (initial TOC: 56.3 ppm; solar irradiation: 36.1 $\mathrm{W\,m^{-2}}$). Recently, Malato Rodríguez et al. [80] reported first results of the photocatalytic degradation of the pollutants of three different wastewaters obtained from chemical companies specialized in the synthesis of phenolic resins (initial TOC: 600, 3600 and 11 800 $\mathrm{mg\,l^{-1}}$) and a distillation effluent (initial TOC: 3–6 $\mathrm{mg\,l^{-1}}$, mainly amino acids, alcohols, and phenols) from a pharmaceutical company, respectively. Degussa P25 or Sachtleben Hombikat UV100 were used as alternative photocatalysts but no significant differences in efficiency were observed. The authors noted that the use of additional oxidants besides air results in a significant increase in the degradation rate with peroxydisulfate being more efficient than hydrogen peroxide [80]. Similar experimental results were obtained by Passarinho et al. [107] who have used CPCRs installed at the

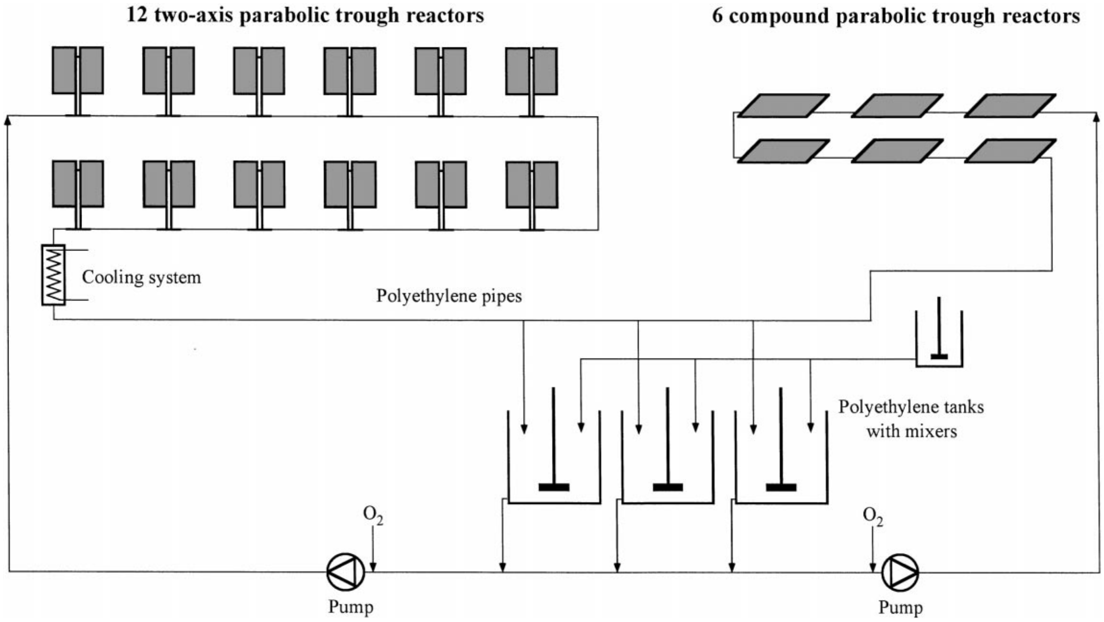

Fig. 11. Flowsheet of the solar photocatalytic detoxification loop installed at the PSA.

PSA to investigate the solar-driven photocatalytic degradation of polyphenols present in olive oil mill wastewaters.

Engineering scale demonstrations of the non-concentrating solar reactor technology were conducted at Tyndall Air Force Base, FL, USA, in 1992 [86,112–115] treating groundwater contaminated with fuel, oil, and lubricants which was leaking from underground storage tanks. Crittenden and co-workers used a tubular photoreactor equipped with reflector and packed with platinized titanium dioxide supported on silica gel. This system was used in a single-pass mode for the photocatalytic degradation of benzene, toluene, ethylbenzene and xylene (BTEX). Without pretreatment fouling of the photocatalyst was observed after less than 1 h of operation. Ionic species were found to be principally responsible for this fouling of the photocatalyst and for the resulting inhibition of the BTEX degradation. A pretreatment unit (filter, oxygenation unit, ion exchanger) was developed to remove ionic species and turbidity and to add oxidants. By using this pretreatment unit, the photocatalytic treatment plant operated efficiently, and no decrease in the photocatalytic activity was observed during 25 days of continuous operation. Even on a rainy day, BTEX compounds ($>2\,\mathrm{mg\,l^{-1}}$ influent concentration) were destroyed within 6.5 min of operation [113].

Goswami and co-workers [114,115] conducted field tests with a slurry tubular reactor without reflector (SOLTOX$^{\mathrm{TM}}$-reactor). Five modules connected in series with a total aperture area of $10\,\mathrm{m}^2$ were used. The photoreactor array was set-up facing south and tilted at an angle of 15° from the horizontal. The experiments were performed in a batch mode by recycling the contaminated groundwater between a tank and the reactor array. While these field tests successfully demonstrated the feasibility of destroying benzene, toluene, ethylbenzene and xylenes (BTEX) in the groundwater, the observed reaction rates were rather low. However, in a laboratory test with city water spiked with the same amounts of BTEX as those present in the groundwater and using the same reactors under similar sunlight conditions, Goswami et al. [115] observed reaction rates which were an order of magnitude higher. These results suggested that a careful site treatability study and the establishment of an appropriate pretreatment will be very important prerequisites for the successful field deployment of solar photocatalytic processes [119]. A very similar pilot plant has been used by Goswami and co-workers [116] for the treatment of a BTEX contaminated groundwater at Gainsville, FL, USA. The flat plate (DSSR) type photoreactor used in this study was developed from a double skinned acrylic panel. The size of the reactor was 1.20 m×2.4 m with a skin thickness of 0.32 cm. The reactor had 39 channels (3 cm×1.3 cm). Headers were made from 0.64 cm thick cylindrical tubes of 3.8 cm inner diameter. The total solar treatment loop (6 reactors and a 1.9 m^3 tank) was operated in a batch mode. The titanium dioxide concentration was 0.1%. Experimental results showed that 1.9 m^3 of water contaminated with 1000 ppb of BTEX can be cleaned reaching a final concentration of 10 ppb in about 3 h provided that an average solar UV energy flux density of 28 $W\,m^{-2}$ is employed [116].

Several reports on the photocatalytic degradation of explosives (e.g., TNT, RDX) present in groundwater and wastewater (“pink water”) using non-solar reactors and artificial illumination have been published recently [120–125], while, however, only two publications have appeared dealing with the solar treatment of this important group of pollutants employing non-concentrating reactors [89,92]. Muradov [92] used a TFFBR (0.8 m^2 surface area, covered with approx. 1.5 $mg\,cm^{-2}$ TiO_2 Degussa P25) for the photocatalytic degradation of nitroglycerine present in contaminated water from a Navy ammunition storage facility. The solar-driven photocatalytic degradation process resulted in a decrease of the nitroglycerine concentration (initially 500 ppm) by more than 99% within 3 h of exposure to the sun (average total solar radiation flux from 900 to 700 $W\,m^{-2}$). Employing the DSSR van Well et al. [89] performed photocatalytic detoxification experiments with groundwater contaminated with nitroaromatic compounds from a World War II-ammunition plant proving that this reactor can indeed be employed for the solar detoxification of such a polluted water stream. Fig. 12 is taken from this work and shows the decrease of the individual concentrations of some nitroaromatic contaminants as a function of the illumination time [89]. More than 75% of all identified contaminants were degraded within 6 h of irradiation and photonic efficiencies similar to those obtained previously in laboratory studies were calculated [124,125].

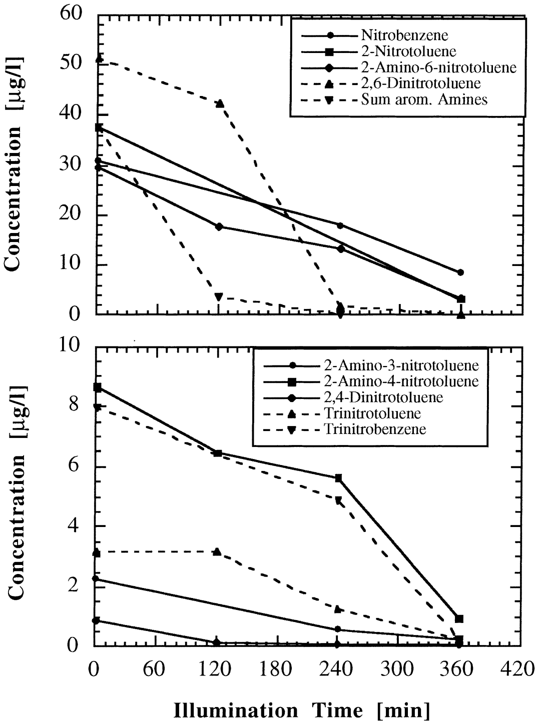

Fig. 12. Photocatalytic degradation of nitroaromatic compounds in a polluted groundwater (Degussa P25, air-saturated suspension, natural pH, ambient temperature, 0.23 m Einstein l^{-1} min^{-1}).

Recently, Dillert et al. [126,127] have treated biologically pretreated industrial wastewaters from the factories Wolfsburg (Germany) and Taubaté (Brazil) of the Volkswagen AG in laboratory and bench-scale experiments. The results of the experiments, which have been performed using the DSSR, were so promising, that a pilot plant was installed in the Wolfsburg factory during the summer 1998 [128]. The flowsheet of this pilot plant is given in Fig. 13, while Fig. 14 shows a photograph of this plant.

This pilot plant which is operated in a recycle batch mode consists of 12 double-skin sheet photoreactors (manufactured by Solacryl) with a total irradiated area of 27.6 m^2. These reactors are connected by a recirculation pipe with a tank (approx. 1.1 m^3 volume). The water (500 l) coming from the biological treatment plant is pumped into the tank and mixed with a catalyst slurry. The solar photocatalytic treatment starts after the tank has been filled.

The suspension (total volume approx. 1 m^3) recycles between the tank and the DSSRs for 8 to 11 h during the daytime. The flow rate out of the tank can

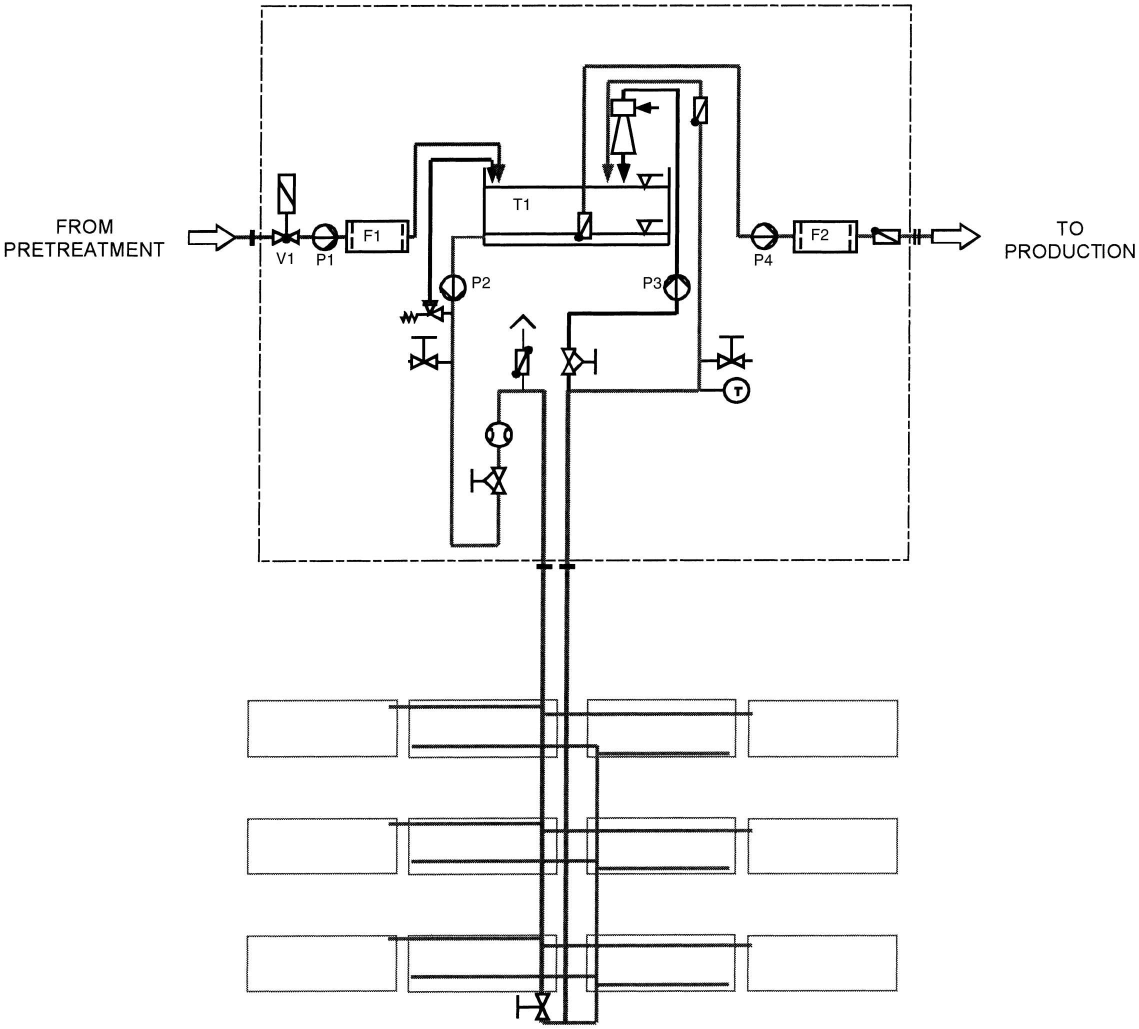

Fig. 13. Flow sheet of the pilot plant for the solar photocatalytic treatment of a biologically pretreated wastewater installed in Wolfsburg, Germany.

be varied between 5000 and 8000 l h^{-1} resulting in a flow rate between 830 and 1300 l h^{-1} in the reactor sheets. After the desired time of the solar photocatalytic treatment the suspension is pumped out of the reactors into the tank. The photocatalyst (5 g l^{-1} Degussa P25) is allowed to settle down during the night. After this sedimentation period the supernatant liquid (500 l) is pumped out of the tank and the treatment cycle can be started again by filling the tank with a new batch of wastewater. The COD and the TOC of the incoming wastewater were determined to vary between 76.6 and 29.0 mg l^{-1} and 26.9 and 10.2 mg l^{-1}, respectively. By mixing the incoming wastewater with the catalyst slurry, which remained in the pilot plant after the supernatant water was pumped out, the COD and the TOC decreased. The initial values of the COD and the TOC were determined to vary between 69.5 and 21.1 mg l^{-1} and 26.9 and 7.3 mg l^{-1}, respectively. During the solar-catalytic treatment a decrease of the concentration of the organic pollutants, determined as COD and TOC, was observed in most cases. As an example, the changes of the UV intensity, COD and TOC during a single run of the pilot plant are given in Fig. 15.

Fig. 14. View on the pilot plant for the solar photocatalytic treatment of a biologically pretreated wastewater installed in Wolfsburg, Germany (Photo: Volkswagen AG).

As a consequence of this oxidation process as well as due to the increase of the reaction temperature, the concentration of molecular oxygen in the reflux pipe between the photoreactors and the tank as well as inside the tank was decreasing. More than 50% of the organic pollutants initially present in the mixed water inside the pilot plant could thus be degraded within 8–11 h of illumination. Naturally, the total mass of the degraded contaminants was found to depend on the initial pollutant concentration, the time of illumination, and, in particular, on the solar UV energy flux density. To analyze the solar experiments performed with this pilot plant the following kinetic expression was used [128]:

$$c = c_0 \exp\left(-\frac{k \times A_R \times \int q_{UV}\,dt}{V_S}\right) \tag{14}$$

with c_0 initial concentration of the wastewater pollutants (determined as TOC or COD), k a kinetic parameter, A_R the total illuminated (light-harvesting) area of the photoreactors, $\int q_{UV}\,dt$ the total UV energy reaching the photoreactors per unit light-harvesting surface area and V_S being the total volume of the suspension in the system. While the values calculated for the TOC reduction (k_{TOC}) (for different catalyst brands and loading as well as for different illuminating conditions) were found to vary between 0.03 and 0.30 $m^3\,kW^{-1}\,h^{-1}$, the values for the COD reduction (k_{COD}) varied between 0.02 and 0.51 $m^3\,kW^{-1}\,h^{-1}$ [128]. The experimental results clearly demonstrate that real wastewater can be successfully treated in solar catalytic treatment plants using titanium dioxide as the photocatalyst. From these results it was predicted that at its final location at the Volkswagen factory in Taubaté (Brazil) this pilot plant will be able to achieve a reduction of the TOC from an initial concentration of 10 $mg\,l^{-1}$ to a final concentration of 1 $mg\,l^{-1}$ when charged with 0.5 m^3 wastewater per day.

Bekbölet et al. [129] have recently applied the photocatalytic degradation process to the destruction of biologically pretreated landfill leachate effluent comparing Sachtleben Hombikat UV100 with

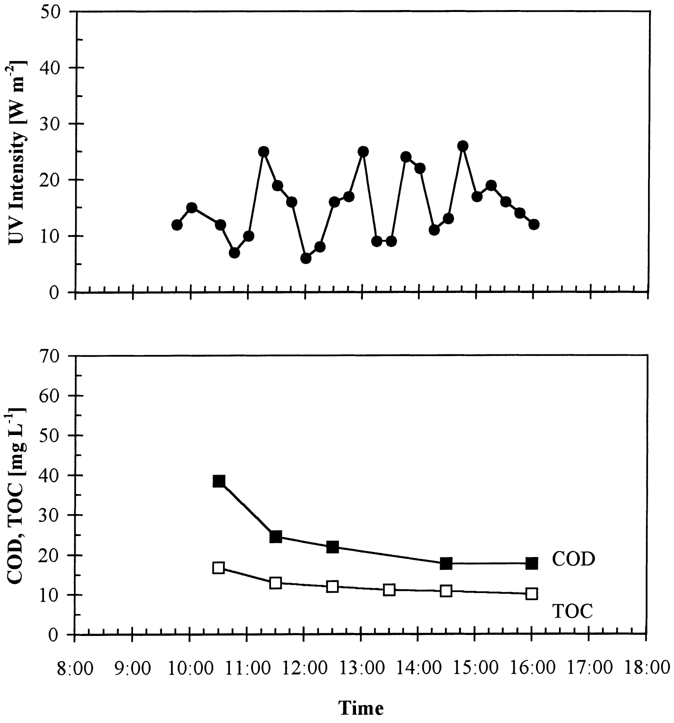

Fig. 15. Change of the solar energy flux density, COD and TOC during a typical run of the solar photocatalytic treatment of a biologically pretreated wastewater installed in Wolfsburg, Germany.

Degussa P25 as potential photocatalyst. These experiments were performed in a batch reactor at pH 3. Both materials, especially Hombikat UV100, showed a strong adsorption of the organic pollutants; the overall TOC-removal was almost the same for both catalysts (≈70%) after 5 h of irradiation with a high-pressure xenon-lamp, the BOD_5 increase was insignificant indicating that the water could still not be treated by conventional biological methods (BOD_5 is defined as the biological oxygen demand during an incubation period of 5 days at 37°C and thus represents a convenient measure for the biodegradability of a real wastewater). In addition to the detoxification experiments, the pH dependent adsorptive properties of the pollutants present in the landfill leachate onto Hombikat UV100 were examined. In good agreement with the pH dependence of the photocatalytic degradation of the leachate, a strong adsorption was observed between pH 3 and 8 with a maximum at pH 5, while at pH 11 the adsorption was much lower [129]. Additional degradation experiments were performed with the TFFBR using Hombikat UV100 coated glass panes irradiated by fluorescent tubes, resembling the UV(A)-portion of the solar spectrum. The highest degradation rate was observed between pH 3 and 7 with a maximum at pH 5, while at pH 9 and 11 the degradation was rather slow. Besides this pH-dependency, the influence of the initial pollutant concentration (dilution of the landfill leachate), the light intensity and the addition of oxidizing reagents (H_2O_2 and $Na_2S_2O_8$) on the degradation rate were examined [129]. A higher rate could be achieved by diluting the leachate, with a maximum rate noted at a moderate dilution (around 1:2 v/v). No beneficial effect was obtained by the addition of H_2O_2 or $Na_2S_2O_8$. The addition of 0.5 or 1 mmol l^{-1} H_2O_2 (at pH 7) even resulted in an inhibition, while in the presence of $Na_2S_2O_8$ (at the same concentration) a dark degradation was observed. Illumination with a reduced light intensity (50 W m^{-2} instead of 100 W m^{-2}) resulted in a lower degradation rate, but a higher photonic efficiency, i.e., a higher efficiency of the process than with maximum light intensity. Finally, the TFFBR system was used in a recirculation mode, and the dependence of the degradation rate on the initial pollutant concentration was examined. The highest photonic efficiency was obtained with undiluted landfill leachate, while the highest relative photodegradation, and therefore the lowest half life of the pollutants was measured with the most diluted sample (1:5 v/v). Photonic efficiency and photoreactor efficiency as well as the kinetic parameters were calculated for the recirculation system. The photonic efficiencies obtained were 0.3–1.0%, i.e., similar to those determined for the single-pass experiments. The relatively low photonic efficiencies for the degradation of the effluent water are not surprising, since it is a well-known fact that the detoxification of real wastewaters by photocatalysis or other chemical oxidation techniques yields considerably lower photonic efficiencies than that of model systems. These observations are, among other things, explained by the presence of inhibiting anions in the real systems [130]. However, it could be shown by the investigation by Bekbölet et al. [129] that photocatalysis is indeed a feasible method for the successful cleaning-up of landfill effluent water. This is especially important as Weichgrebe [131,132] could demonstrate that by photocatalysis higher rates can be obtained for the degradation of landfill leachate than with other, more conventional wet oxidation methods (e.g., ozone or hydrogen peroxide coupled with UV- irradiation).

Recently, Freudenhammer et al. [133] reported their results from a pilot study using TFFBR reactors which was performed in various Mediterranean countries and showed that biologically pretreated textile wastewater can be cleaned by solar photocatalysis with a maximum degradation rate of 3 g COD h^{-1} m^{-2}. Moreover, a comparison of reaction rates measured under artificial and under solar illumination, respectively, which was also performed during this study proved the necessity of outdoor experiments. It was concluded that photocatalysis should be a suitable technology as the final stage of purification of biologically or physically pretreated wastewater in particular in sun-rich areas. However, it was also pointed out that industrial applications of solar wastewater treatment on a larger scale is in strong demand for cheap photocatalysts of higher activity to be competitive with treatment methods already established on the market [133].

Other investigations of real industrial wastewater treatment which have, however, not yet been conducted at an engineering scale demonstrate the potential of the solar photocatalytic water treatment process especially for problematic waters where conventional treatment methods are not successful. Thus, the applicability of the solar photocatalytic oxidation could be shown for the treatment of wastewater from a 5-fluorouracil (a cancer drug) manufacturing plant [134]. Moreover, a simultaneous color and COD reduction was observed during the photocatalytic treatment of a distillery wastewater that had been pretreated by anaerobic microbiological methods [135]. A laboratory study conducted by Turchi and Ollis [136] has furthermore shown that wastewater from pulp and paper mills can also be treated conveniently by photocatalysis.

3.5. Economic considerations

In most cases the economics of the solar photocatalytic applications will determine the commercial viability of this process. According to Goswami [119,137] an economic analysis should include the fixed capital costs, recurring operation and maintenance costs, as well as energy costs. Ollis [138] presented an early comparative economic assessment of water purification by photocatalysis employing UV-lamps, UV-ozone technology and activated carbon adsorption technology. He concluded that the cost of treating contaminated water by the UV-photocatalytic system already approaches the treatment cost of the activated carbon system provided that the costs of spent carbon disposal are included. Turchi and Link [139] conducted a comparative economic assessment of water treatment by solar photocatalysis (employing PTR reactors), activated carbon adsorption, and UV-hydrogen peroxide technology. They concluded that a fivefold decrease of the costs of solar water treatment would be required for this technology to be economically competitive with the established technologies and subsequently showed that such a cost reduction can be achieved by the deployment of non-concentrating solar reactors [140]. In a recent review Goswami [119] reported cost calculations for the solar photocatalytic wastewater treatment ranging from US \$0.53 m^{-3} all the way to US \$27.57 m^{-3} based upon various literature sources. Obviously, the predicted treatment cost will strongly depend upon the type of wastewater, the desired mode of plant operation (i.e., continuous vs. discontinuous), the location of the projected plant, and a variety of other individual factors. Thus, in each case an individual economic assessment will be required based upon reliable experimental data, which have to be obtained under realistic operating conditions to be able to compare the costs with traditional technologies. Moreover, whenever the costs of the activated carbon adsorption are used for such a comparison it will be important to include also the costs for an environmentally safe disposal of the used and thus often highly contaminated carbon adsorber.

It has been shown that the costs of the photocatalytic reactors are contributing the main part to the overall treatment costs [137]. In many cases the cost of the land area required for the installation of a solar water detoxification plant will add a significant portion to the overall costs of the process. Therefore, it is important to calculate the required illuminated reactor area as accurately as possible.

Based on the efficiencies determined for solar detoxification reactors, van Well et al. [89] have recently presented a calculation of the reactor area required for a given pollution problem. Taking a continuous flow reactor and typical solar UV-A light intensities the authors assumed a zero order reaction (in concentrations) with the rate being directly proportional to the light intensity I and the illuminated surface of the photoreactor A. Considering a total degradation of the contaminants they calculated the required illuminated reactor area A as a function of the incoming molar flow rate of the water pollutant(s) ($\dot{n}_{\mathrm{in}}$), assuming a light intensity I (actually a radiation flux) of 60 μmol photons m^{-2} s^{-1} and different photonic efficiencies [89]. Taking an incoming molar flow rate of $\dot{n}_{\mathrm{in}}$ of 0.6 mmol l^{-1} s^{-1} (i.e., about 0.22 mol m^{-3} h^{-1}) these calculations showed that a total reactor area of 102.9 m^2 will be required at a flow rate of 10 m^3 h^{-1} assuming a photonic efficiency of ζ=0.1 [89]. This could, e.g., be realized by a cascade of 75 Plexiglas® DSSR. A straightforward calculation evinces that this area requirement will have to be multiplied by a factor of 2.3 or 4.6, respectively, when the destruction of the contaminants follows first order kinetics and 90 or 99% degradation, respectively, is the desired result.

4. Conclusions

The following conclusions summarize our views concerning photocatalytic reactors and respective solar technologies:

1. Methods are now available for the correct evaluation of true photon absorption rates in the most commonly used reactor geometries.
2. It is clear that the evaluation of the absorbed light in suspended solid photocatalytic systems must take into account scattering.
3. Photocatalytic processes employing solar illumination and slurry reactor operation have shown to be a feasible technology for the treatment of small to medium volumes of wastewaters. The volume limitation mainly originates from the necessary separation of the suspended catalyst after treatment.
4. Flat plate reactors are an attractive design because their efficiency is at least equal to other reactor configurations and their construction offers economic advantages.
5. Much work is needed to develop more precise methods for modeling the kinetics of real wastewaters systems and to incorporate into them realistic irradiation rates that are strongly dependent on time and the prevailing weather conditions.
6. Photocatalytic technologies for water and wastewater applications, either using artificial or solar light, will advantageously compete in the market, in particular, if more efficient catalysts are developed.

5. Nomenclature

A	area (m^2)
A_{R}	photoreactor light harvesting area (m^2)
A_{T}	total light harvesting area (m^2)
c	pollutant concentration (mol m^{-3} or mol l^{-1})
c_0	initial pollutant concentration (mol m^{-3} or mol l^{-1})
C_{c}	catalyst concentration (g m^{-3})
e^{a}	local volumetric rate of radiant energy absorption (Einstein m^{-3} s^{-1})
$E_{\mathrm{UV,tot}}$	$\int_t q_{\mathrm{UV}}\,\mathrm{d}t$, total collected radiation energy per unit area (J m^{-2})
G	incident radiation (Einstein m^{-2} s^{-1})

I	spectral radiation specific intensity (Einstein $\mathrm{m^{-2}\,sr^{-1}\,s^{-1}}$)
k	kinetic parameter ($\mathrm{m^3\,kW^{-1}\,h^{-1}}$)
M	measurement of radiation flux ($\mathrm{W\,m^{-2}}$)
n_a	number of absorbed photons by the photocatalyst (photons)
$\dot{n}_\mathrm{in}$	molar flow rate ($\mathrm{mmol\,l^{-1}\,s^{-1}}$)
n_ph	number of photons potentially absorbable by the photocatalyst (photons)
p	phase function (dimensionless)
q	radiative density flux (Einstein $\mathrm{m^{-2}\,s^{-1}}$ or $\mathrm{W\,m^{-2}}$)
r	cylindrical radial coordinate (m)
R	catalyst reflectivity (dimensionless)
R_eff	effective degradation rate ($\mathrm{mg\,m^{-2}\,h^{-1}}$)
$\mathfrak{R}$	reaction parameter ($\mathrm{mol\,m^{-2}\,s^{-1}}$)
r_2	reactor external radius (m)
s	linear coordinate along the direction $\underline{\Omega}$ (m)
S	mass/area ratio ($\mathrm{mg\,m^{-2}}$)
t	time (s or h)
TOC	total organic carbon (mg)
V	reactor volume ($\mathrm{m^3}$)
V_S	total suspension volume ($\mathrm{m^3}$)
V_T	total reactor volume ($\mathrm{m^3}$ or l)
x	axial coordinate (m)
$\underline{x}$	spatial position vector (m)
z	cylindrical axial coordinate (m)

Greek letters

α	constant that relates the incident radiation with the radiation flux ($\mathrm{m^{-1}}$)
β	volumetric extinction coefficient ($\mathrm{m^{-1}}$)
β^*	mass extinction coefficient ($\mathrm{m^2\,g^{-1}}$)
θ	spherical coordinate (rad)
κ	volumetric absorption coefficient ($\mathrm{m^{-1}}$)
κ	also, reactor parameter ($\mathrm{m^2\,m^3}$) [62]
κ^*	mass absorption coefficient ($\mathrm{m^2\,g^{-1}}$)
λ	wavelength (nm)
η	solar reactor efficiency ($\mathrm{mg\,J^{-1}}$)
μ	the quantity $\cos\theta$ (dimensionless)
σ	volumetric scattering coefficient ($\mathrm{m^{-1}}$)
ζ	apparent photonic efficiency (mol $\mathrm{Einstein^{-1}}$)
ϕ	spherical coordinate (rad); also fraction of the light absorbed by the catalyst
$\underline{\Omega}$	unit vector in the direction of radiation propagation (dimensionless)
Ω	solid angle (sr)

Subscripts

a	absorbed radiation
i	incident radiation
in	relative to the inner wall
0	relative to the surface of radiation entrance or initial concentration
ou	relative to the outer wall
r	reflected radiation
t	transmitted radiation
w	value at the reactor wall
λ	a dependence on the wavelength

Acknowledgements

Two of us (OMA and AEC) gratefully acknowledge the financial support of Universidad Nacional del Litoral, Consejo Nacional de Investigaciones Científicas y Técnicas and Agencia Nacional de Promoción Científica y Tecnológica of Argentina. The traveling grants provided by KfK (Germany)–SECyT (Argentina) bilateral cooperation agreement, as well as the Alexander von Homboldt Foundation and ISFH solicitous hospitality for AEC are also acknowledged.

References

[1] A.M. Braun, L. Jakob, E. Oliveros, C.A. Oller do Nascimento, Adv. Photochem. 18 (1993) 235.
[2] O. Legrini, E. Oliveros, A.M. Braun, Chem. Rev. 93 (1993) 671.
[3] D. Bahnemann, J. Cunningham, M.A. Fox, E. Pelizzetti, P. Pichat, N. Serpone, in: G.R. Helz, R.G. Zepp, D.G. Crosby (Eds.), Aquatic and Surface Photochemistry, Lewis Publishers, Boca Raton, FL, 1994, p. 261.
[4] M.R. Hoffmann, S.T. Martin, W. Choi, D.W. Bahnemann, Chem. Rev. 95 (1995) 69.
[5] D. Bahnemann, in: P. Boule (Ed.), The Handbook of Environmental Chemistry, Part I, Vol. 2, Environmental Photochemistry, Springer, Berlin, 1999, p. 285.
[6] S.N. Frank, A.J. Bard, J. Phys. Chem. 81 (1977) 1484.
[7] E. Borgarello, J. Kiwi, E. Pellizzetti, M. Visca, M. Grätzel, J. Am. Chem. Soc. 103 (1981) 6324.
[8] P.A. Brugger, P. Cuendet, M. Grätzel, J. Am. Chem. Soc. 103 (1981) 2923.
[9] L.P. Childs, D.F. Ollis, J. Catal. 66 (1980) 383.

[10] A.L. Prudent, D.F. Ollis, J. Catal. 82 (1983) 404.
[11] C.Y. Hsiao, C.L. Lee, D.F. Ollis, J. Catal. 82 (1983) 418.
[12] D.F. Ollis, C.Y. Hsiao, L. Budiman, C.L. Lee, J. Catal. 88 (1984) 89.
[13] M. Schiavello (Ed.), Photoelectrochemistry, Photocatalysis and Photoreactors, Reidel, Dordrecht, 1985.
[14] E. Pellizzetti, N. Serpone (Eds.), Homogeneous and Heterogeneous Photocatalysis, Reidel, Dordrecht, 1986.
[15] M. Schiavello (Ed.), Photocatalysis and Environment, Kluwer Academic Publishers, Dordrecht, 1988.
[16] N. Serpone, E. Pellizzetti (Eds.), Photocatalysis: Fundamentals and Applications, Wiley, New York, 1989.
[17] E. Pellizzetti, M. Schiavello (Eds.), Photochemical Conversion and Storage of Solar Energy, Kluwer Academic Publishers, Dordrecht, 1991.
[18] D.F. Ollis, H. Al-Ekabi (Eds.), Photocatalytic Purification and Treatment of Water and Air, Elsevier, Amsterdam, 1993.
[19] R.W. Matthews, Water Res. 20 (1986) 569.
[20] R.W. Matthews, J. Phys. Chem. 91 (1987) 3328.
[21] R.W. Matthews, J. Catal. 111 (1988) 264.
[22] R.W. Matthews, J. Catal. 113 (1988) 549.
[23] D.F. Ollis, E. Pellizzetti, N. Serpone, Environ. Sci. Technol. 25 (1991) 1522.
[24] A.E. Cassano, O.M. Alfano, this issue.
[25] O.M. Alfano, R.L. Romero, A.E. Cassano, Chem. Eng. Sci. 41 (1986) 1137.
[26] A.E. Cassano, C.A. Martín, R.J. Brandi, O.M. Alfano, Ind. Eng. Chem. Res. 34 (1995) 2155.
[27] M.I. Cabrera, O.M. Alfano, A.E. Cassano, J. Phys. Chem. 100 (1996) 20043.
[28] S. Esplugas, S. Cervera, R. Simarro, Chem. Eng. Commun. 51 (1987) 221.
[29] M. Schiavello, V. Augugliaro, L. Palmisano, J. Catal. 127 (1991) 332.
[30] V. Augugliaro, L. Palmisano, M. Schiavello, AIChE J. 37 (1991) 1096.
[31] P.L. Yue, in: D.F. Ollis, H. Al-Ekabi (Eds.), Photocatalytic Purification and Treatment of Water and Air, Elsevier, Amsterdam, 1993, p. 495.
[32] J. Lea, A.A. Adesina, J. Photochem. Photobiol. A 118 (1998) 111.
[33] L. Davydov, P.G. Smirniotis, S.E. Pratsinis, Ind. Eng. Chem. Res. 38 (1999) 1376.
[34] L. Rideh, A. Wehrer, D. Ronze, A. Zoulalian, Catal. Today 48 (1999) 357.
[35] D.F. Ollis, C. Turchi, Environ. Prog. 9 (4) (1990) 229.
[36] P. Pichat, Catal. Today 19 (1994) 313.
[37] P. Pichat, in: M. Schiavello (Ed.), Photoelectrochemistry, Photocatalysis and Photoreactors, Reidel, Dordrecht, 1985, p. 425.
[38] C.S. Turchi, D.F. Ollis, J. Catal. 119 (1989) 483.
[39] A.L. Pruden, D.F. Ollis, J. Catal. 82 (1983) 404.
[40] D. Bahnemann, D. Bockelmann, R. Goslich, Solar Energy Mater. 24 (1991) 564.
[41] A. Sclafani, A. Brucato, L. Rizzuti, in: D.F. Ollis, H. Al-Ekabi (Eds.), Photocatalytic Purification and Treatment of Water and Air, Elsevier, Amsterdam, 1993, p. 533.
[42] A. Brucato, L. Rizzuti, Ind. Eng. Chem. Res. 36 (1997) 4740.
[43] A. Brucato, L. Rizzuti, Ind. Eng. Chem. Res. 36 (1997) 4748.
[44] T. Yokota, Y. Takahata, H. Nanjo, K. Takahashi, J. Chem. Eng. Jpn. 22 (1989) 537.
[45] T. Yokota, Y. Takahata, J. Hosoya, K. Suzuki, K. Takahashi, J. Chem. Eng. Jpn. 22 (1989) 543.
[46] T. Yokota, Y. Takahata, Y. Ohto, K. Takahashi, J. Chem. Eng. Jpn. 22 (1989) 548.
[47] S. Cervera, J. Giménez, D. Curcó, X. Domènech, J. Peral, Proc. Electrochem. Soc. 94 (1994) 255.
[48] M. Pasquali, F. Santarelli, J.F. Porter, P.L. Yue, AIChE J. 42 (1996) 532.
[49] G. Spadoni, E. Bandini, F. Santarelli, Chem. Eng. Sci. 33 (1978) 517.
[50] C.A. Martín, M.A. Baltanás, A.E. Cassano, Catal. Today 27 (1996) 221.
[51] C.A. Martín, M.A. Baltanás, A.E. Cassano, J. Photochem. Photobiol. A 94 (1996) 173.
[52] C.A. Martín, M.A. Baltanás, A.E. Cassano, Environ. Sci. Technol. 30 (1996) 2355.
[53] O.M. Alfano, A.C. Negro, M.I. Cabrera, A.E. Cassano, Ind. Eng. Chem. Res. 34 (1995) 488.
[54] M.I. Cabrera, O.M. Alfano, A.E. Cassano, Ind. Eng. Chem. Res. 34 (1995) 500.
[55] O.M. Alfano, M.I. Cabrera, A.E. Cassano, Chem. Eng. Sci. 49 (1994) 5327.
[56] M.I. Cabrera, O.M. Alfano, A.E. Cassano, Ind. Eng. Chem. Res. 33 (1994) 3031.
[57] M.I. Cabrera, O.M. Alfano, A.E. Cassano, J. Catal. 173 (1997) 380.
[58] O.M. Alfano, M.I. Cabrera, A.E. Cassano, J. Catal. 173 (1997) 370.
[59] R.J. Brandi, O.M. Alfano, A.E. Cassano, Chem. Eng. Sci. 51 (1996) 3169.
[60] R.J. Brandi, O.M. Alfano, A.E. Cassano, Chem. Eng. Sci. 54 (13–14) (1999) 2817.
[61] R.L. Romero, O.M. Alfano, A.E. Cassano, Ind. Eng. Chem. Res. 36 (1997) 3094.
[62] L. Jakob, E. Oliveros, O. Legrini, A.M. Braun, in: D.F. Ollis, H. Al-Ekabi (Eds.), Photocatalytic Purification and Treatment of Water and Air, Elsevier, Amsterdam, 1993, p. 511.
[63] A.K. Ray, A.A.C.M. Beenackers, AIChE J. 44 (2) (1998) 477.
[64] A.K. Ray, Catal. Today 44 (1998) 357.
[65] P.S. Mukherjee, A.K. Ray, Chem. Eng. Technol. 22 (3) (1999) 253.
[66] L. Puma, P.L. Yue, Chem. Eng. Sci. 53 (1998) 2993.
[67] L. Puma, P.L. Yue, Chem. Eng. Sci. 53 (1998) 3007.
[68] D.M. Blake, H. Link, K. Eber, in: K.W. Böer (Ed.), Advances in Solar Energy, Vol. 7, American Solar Energy Society, Boulder, CO, USA, 1992, p. 167.
[69] C. Turchi, M. Mehos, J. Pacheco, in: D.F. Ollis, H. Al-Ekabi (Eds.), Photocatalytic Purification and Treatment of Water and Air, Trace Metals in the Environment, Vol. 3, Elsevier, Amsterdam, 1993, p. 789.
[70] K. Pacheco, A.S. Watt, C.S. Turchi, in: Proceedings of the ASME/ASES Joint Solar Engineering Conference, New York, 1993, p. 43.

[71] D.Y. Goswami, in: K.W. Böer (Ed.), Advances in Solar Energy, Vol. 10, American Solar Energy Society, Boulder, CO, USA, 1995, p. 165.
[72] J. Sabate, M.A. Anderson, M.A. Aguado, J. Gimenez, S. Cervera-March, C.G.J. Hill, Mol. Catal. 71 (1992) 57.
[73] R.W. Matthews, S.R. McEvoy, J. Photochem. Photobiol. A 64 (1992) 231.
[74] G. Chester, M.A. Anderson, H. Read, S. Esplugas, J. Photochem. Photobiol. A 71 (1993) 291.
[75] M. Bideau, B. Claudel, C. Dubien, L. Faure, H. Kazouan, J. Photochem. Photobiol. A 91 (1995) 137.
[76] R. Pozzo, M.A. Baltanás, A.E. Cassano, Catal. Today 54 (1999) 143.
[77] J.E. Pacheco, C.E. Tyner, Solar Engineering 1990, in: Proceedings of the ASME Solar Energy Conference, Miami, p. 163.
[78] J.E. Pacheco, J.T. Holmes, ACS Symp. Ser. 422 (1990) 40.
[79] Final Configuration of PSA solar detoxification loop, Plataforma Solar de Almería TRO6/91, 1991.
[80] S. Malato Rodríguez, C. Richter, J. Blanco Gálvez, M. Vincent, Solar Energy 56 (1996) 401.
[81] J. Giménez, D. Curcó, S. Malato, J. Blanco, L. Borrell, P. Marco, in: M. Becker, M. Böhmer (Eds.), Solar Thermal Concentrating Technologies, Proceedings of the Eighth International Symposium, Vol. 3, Müller, Heidelberg, 1997, p. 1431.
[82] Y. Zhang, J.C. Crittenden, D.W. Hand, D.L. Perram, Environ. Sci. Technol. 28 (1994) 435.
[83] N.J. Peill, M.R. Hoffmann, J. Solar Energy Eng. 119 (1997) 229.
[84] G. Cooper, M.A. Ratcliff, US Patent 451375 (1989).
[85] J. Bedford, J.F. Klausner, D.Y. Goswami, K.S. Schanze, J. Solar Energy Eng. 116 (1994) 8.
[86] V. Öberg, D.Y. Goswami, G. Svedberg, Solar Engineering 1993, in: Proceedings of the ASME International Solar Energy Conference, Washington, p. 147.
[87] P. Wyness, J.F. Klausner, D.Y. Goswami, K.S. Schanze, J. Solar Energy Eng. 116 (1994) 2.
[88] V. Benz, M. Müller, D. Bahnemann, D. Weichgrebe, M. Brehm, Deutsche Offenlegungsschrift DE 19514372 Al, October 10, 1996.
[89] M. van Well, R.H.G. Dillert, D.W. Bahnemann, V.W. Benz, M.A. Mueller, J. Solar Energy Eng. 119 (1997) 114.
[90] M. Hilgendorff, D. Bockelmann, R.F.P. Nogueira, D. Weichgrebe, W.F. Jardim, D. Bahnemann, R. Goslich, in: Proceedings of the Sixth International Symposium on Solar Thermal Concentrating Technologies, Mojácar, 1992 Editorial CIEMAT: Madrid 1993, Vol. 2, p. 1167.
[91] R.F.P. Nogueira, W.F. Jardim, Solar Energy 56 (1996) 471.
[92] N.Z. Muradov, Solar Energy 52 (1994) 283.
[93] R.E. Bird, R.L. Hulstrom, L.J. Lewis, Solar Energy 30 (1983) 563.
[94] J.E. Pacheco, M.R. Prairie, L. Yellowhorse, J. Solar Energy Eng. 115 (1993) 123.
[95] C.S. Turchi, M.S. Mehos, Chem. Oxid.: Technologies for the nineties. Proc. 2nd Int. Sym., Nashville, 1992. Technomic Publ., Lancaster. (1994) 301
[96] J.E. Pacheco, M. Mehos, C. Turchi, H. Link, in: D.F. Ollis, H. Al-Ekabi (Eds.), Photocatalytic Purification and Treatment of Water and Air, Trace Metals in the Environment, Vol. 3, Elsevier, Amsterdam, 1993, p. 547.
[97] M.S. Mehos, C.S. Turchi, Environ. Prog. 12 (1993) 194.
[98] C. Minero, E. Pelizzetti, S. Malato, J. Blanco, Chemosphere 26 (1993) 2103.
[99] J. Blanco, S. Malato, Solar Engineering 1994, in: Proceedings of the ASME/JSME/JSES Joint Solar Engineering Conference, San Francisco p. 103.
[100] J. Blanco, S. Malato, D. Bahnemann, D. Bockelmann, D. Weichgrebe, R. Goslich, F. Carmona, F. Martinez, in: Proceedings of the Seventh International Symposium on Solar Thermal Concentrating Technologies, Moscow, 1994.
[101] S. Malato, J. Blanco, C. Richter, D. Curco, J. Giménez, Water Sci. Technol. 35 (1997) 157.
[102] C. Richter, S. Malato Rodríguez, J. Blanco Gálvez, in: M. Becker, M. Böhmer (Eds.), Solar Thermal Concentrating Technologies, Proceedings of the Eighth International Symposium, Vol. 3, Müller, Heidelberg, 1997, p. 1521.
[103] D. Bockelmann, R. Goslich, D. Weichgrebe, D. Bahnemann, in: D.F. Ollis, H. Al-Ekabi (Eds.), Photocatalytic Purification and Treatment of Water and Air, Trace Metals in the Environment, Vol. 3, Elsevier, Amsterdam, 1993, p. 771.
[104] D. Bockelmann, Solare Reinigung verschmutzter Wässer mittels Photokatalyse, Thesis, Universität Clausthal-Zellerfeld, 1993, Cuvillier, Göttingen, 1994.
[105] D. Bockelmann, D. Weichgrebe, R. Goslich, D. Bahnemann, Solar Energy Mater. Solar Cells 38 (1995) 441.
[106] A. Vidal, J.I. Ajona, J. Blanco, M. Romero, I. Muguruza, A. Díaz, M. Zallo, J. Gonzales, in: M. Becker, M. Böhmer (Eds.), Solar Thermal Concentrating Technologies, Proceedings of the Eighth International Symposium, Vol. 3, Müller, Heidelberg, 1997, p. 1365.
[107] P.C. Passarinho, A.S. Vieira, S. Malato Rodríguez, J. Blanco Gálvez, in: Proceedings of the First Users Workshop Training and Mobility of Researchers Programme at Plataforma Solar de Almerìa, Almerìa, Spain, November 18–19, 1997, Editorial CIEMAT, Madrid, 1998, p. 7.
[108] J. Giménez, M.A. Queral, D. Curcú, in: Proceedings of the First Users Workshop Training and Mobility of Researchers Programme at Plataforma Solar de Almerìa, Almerìa, Spain, November 18–19, 1997, Editorial CIEMAT, Madrid, 1998, p. 19.
[109] R. Goslich, D. Bahnemann, H.-W. Schumacher, V. Benz, M. Müller, in: M. Becker, M. Böhmer (Eds.), Solar Thermal Concentrating Technologies, Proceedings of the Eighth International Symposium, Vol. 3, Müller, Heidelberg, 1997, p. 1337.
[110] R. Dillert, R. Goslich, J. Dzengel, H.-W. Schumacher, D. Bahnemann, in: Proceedings of the First Users Workshop Training and Mobility of Researchers Programme at Plataforma Solar de Almerìa, Almerìa, Spain, November 18–19, 1997, Editorial CIEMAT, Madrid, 1998, p. 31.
[111] D. Bahnemann, R. Dillert, J. Dzengel, R. Goslich, G. Sagawe, H.-W. Schumacher, J. Adv. Oxid. Technol. 4 (1999) 11.

[112] J.C. Crittenden, Y. Zhang, D.W. Hand, D.L. Perram, E.G. Marchand, Water Environ. Res. 68 (1996) 270.

[113] Y. Zhang, J.C. Crittenden, D.W. Hand, D.L. Perram, J. Solar Energy Eng. 118 (1996) 123.

[114] C.S. Turchi, J.F. Klausner, D.Y. Goswami, E. Marchand, Chem. Oxid.: Technologies for the nineties. Proc. 3rd Int. Symp., Nashville, 1993. Technomic Publ., Lancaster (1994) 216.

[115] D.Y. Goswami, J. Klausner, G.D. Marthur, A. Martin, K. Schanze, P. Wyness, C. Turchi, E. Marchand, Solar '93, Proceedings of the 1993 Annual Conference of the American Solar Energy Society, Washington, p. 235.

[116] M. Srinivasan, J.F. Klausner, C.K. Jotshi, D.Y. Goswami, in: ASME International Solar Energy Conference, Orlando, FL, USA, 1997.

[117] D. Bockelmann, Deutsche Offenlegungsschrift P 42373905 (1993).

[118] M. Lindner, D.W. Bahnemann, B. Hirthe, W.D. Griebler, J. Solar Energy Eng. 119 (1997) 120.

[119] D.Y. Goswami, J. Solar Energy Eng. 119 (1997) 101.

[120] D.M. Blake, E. Wolfrum, J. Boulter, M. Prairie, S. Showalter, P. Rodacy, P. Leslie, B. Stange, Photocatalytic oxidation and reduction chemistry and a new process for treatment of pink water and related contaminated water, National Renewable Energy Laboratory, Report NREL/TP-430-2 1580, 1996.

[121] P.J. Rodacy, P.K. Leslie, M.R. Prairie, B. Stange, S. Showalter, C.L. Renschler, C.A. White, R. Buss, R. Sierka, C. Bryant, Destruction of explosives in groundwater and process water using photocatalytic and biological methods, Sandia National Laboratories, Report SAND96-0929, 1996.

[122] Z. Wang, C. Kutal, Chemosphere 30 (1995) 1125.

[123] D.C. Schmelling, K.A. Gray, Water Res. 29 (1995) 2651.

[124] R. Dillert, M. Brandt, I. Fornefett, U. Siebers, D. Bahnemann, Chemosphere 30 (1995) 2333.

[125] R. Dillert, I. Fornefett, U. Siebers, D. Bahnemann, J. Photochem. Photobiol. A 94 (1996) 231.

[126] R. Dillert, S. Vollmer, M. Schober, J. Theurich, D. Bahnemann, H.-J. Arntz, K. Pahlmann, J. Wienefeld, T. Schmedding, G. Sager, gwf Wasser Abwasser 140 (1999) 293.

[127] R. Dillert, S. Vollmer, M. Schober, J. Theurich, D. Bahnemann, H.-J. Arntz, K. Pahlmann, J. Wienefeld, T. Schmedding, G. Sager, Chem. Ing. Technol. 71 (1999) 396.

[128] R. Dillert, S. Vollmer, E. Gross, M. Schober, D. Bahnemann, J. Wienefeld, K. Pahlmann, T. Schmedding, H.-J. Arntz, G. Sager, Z. Phys. Chem. 213 (1999) 141.

[129] M. Bekbölet, M. Lindner, D. Weichgrebe, D.W. Bahnemann, Solar Energy 56 (1996) 455.

[130] M. Lindner, J. Theurich, D.W. Bahnemann, Water Sci. Technol. 35 (1997) 79.

[131] D. Weichgrebe, A. Vogelpohl, D. Bockelmann, D. Bahnemann, in: D.F. Ollis, H. Al-Ekabi (Eds.), Photocatalytic Purification and Treatment of Water and Air, Trace Metals in the Environment, Vol. 3, Elsevier, Amsterdam, 1993, p. 579.

[132] D. Weichgrebe, Beitrag zur chemisch-oxidativen Abwasserbehandlung, Cuvillier Verlag, Göttingen, 1994.

[133] H. Freudenhammer, D. Bahnemann, L. Bousselmi, S.-U. Geissen, A. Ghrabi, F. Saleh, A. Si-Salah, U. Siemon, A. Vogelpohl, Water Sci. Technol. 35 (1997) 149.

[134] M. Anheden, D.Y. Goswami, G. Svedberg, J. Solar Energy Eng. 118 (1996) 2.

[135] A.H. Zaidi, D.Y. Goswami, A.C. Wilkie, in: Proceedings of the American Solar Energy Society Annual Conference, Minneapolis, 1995, p. 235.

[136] C.S. Turchi, D.F. Ollis, J. Catal. 119 (1989) 483.

[137] D.Y. Goswami, S.K. Sharma, G.D. Mathur, C.K. Jotshi, J. Solar Energy Eng. 119 (1997) 108.

[138] D.F. Ollis, NATO ASI Series, Series C, Photocatal. Environ. 237 (1988) 663.

[139] C.S. Turchi, H.F. Link, Solar Engineering 1991, in: Proceedings of the 1991 ASME/JSES/JSME International Solar Energy Conference, Reno, p. 289.

[140] C.S. Turchi, H.F. Link, in: Proceedings of the 1991 Solar World Congress International Solar Energy Society, Denver, CO, USA.